Research article

urn:lsid:zoobank.org:pub:03800D6D-8743-4194-BEB9-12264B3BC41C

A new species of *Odontophrynus* (Anura, Odontophrynidae) from the southern portion of the Mantiqueira mountains

Matheus de Toledo MOROTI [1], Mariana PEDROZO [2,*], Marcos Rafael SEVERGNINI [3],
Guilherme AUGUSTO-ALVES [4], Simone DENA [5], Itamar Alves MARTINS [6],
Ivan NUNES [7] & Edelcio MUSCAT [8]

[1,2,8] Projeto Dacnis. Estrada do Rio Escuro, 4754, Sertão das Cotias, CEP 11680-000,
Ubatuba, São Paulo, Brazil.
[1,3] Programa de Pós-Graduação em Ecologia e Conservação, Instituto de Biociências,
Universidade Federal de Mato Grosso do Sul (UFMS), Cidade universitária, CEP 79002-970,
Campo Grande, Mato Grosso do Sul, Brazil.
[4] Laboratório de História Natural de Anfíbios Brasileiros (LaHNAB), Departamento de Biologia
Animal, Instituto de Biologia, Universidade Estadual de Campinas (UNICAMP),
Cidade Universitária, CEP 13083-862, Campinas, São Paulo, Brazil.
[4] Programa de Pós-Graduação em Ecologia, UNICAMP, Instituto de Biologia,
Cidade Universitária, CEP 13083-865, Campinas, São Paulo, Brazil.
[5] Fonoteca Neotropical Jaques Vielliard (FNJV), Museu de Diversidade Biológica - MDBio – Área
Zoologia, Instituto de Biologia, UNICAMP, CEP 13083-862, Campinas, São Paulo, Brazil.
[6] Laboratório de Zoologia, Universidade de Taubaté (UNITAU), CEP 12030-180,
Taubaté, São Paulo, Brazil.
[7] Laboratório de Herpetologia (LHERP), Instituto de Biociências, Campus do Litoral Paulista,
Universidade Estadual Paulista (UNESP), CEP 11330-900, São Vicente, São Paulo, Brazil.

*Corresponding author: mariana.pedrozo.24@gmail.com
[1] Email: mmoroti@gmail.com
[3] Email: marcosrafaelsevergnini@gmail.com
[4] Email: alves.guilherme.augusto@gmail.com
[5] Email: sdena@unicamp.br
[6] Email: itamarmartins1@gmail.com
[7] Email: ivan.nunes@unesp.br
[8] Email: edelciomuscat@terra.com.br

[1] urn:lsid:zoobank.org:author:B26E6F24-BC63-4521-910D-6452C5348967
[2] urn:lsid:zoobank.org:author:42B796D8-4269-403F-ACA6-9700946E540F
[3] urn:lsid:zoobank.org:author:B2ED02E8-59C3-4055-B51D-E37AC5FD125A
[4] urn:lsid:zoobank.org:author:FC1879FC-6401-4A35-AA8F-D329EC85DBB8
[5] urn:lsid:zoobank.org:author:53AEC799-BD04-4D5E-AC7D-DCFE3A454983
[6] urn:lsid:zoobank.org:author:5DABF971-76C6-4EEA-8A6B-96DCEBF84046
[7] urn:lsid:zoobank.org:author:1B9148F5-007E-4465-8988-DACB63207E35
[8] urn:lsid:zoobank.org:author:FE9F1DCE-6EAA-462B-81DF-C76275DC0B2C

Abstract. Using an integrative approach (morphology of the adult and larvae, bioacoustics, osteology, karyotype, and molecular data), we described a new tetraploid species of *Odontophrynus* to the Mantiqueira mountain range, in southeastern Brazil. The data suggest that *Odontophrynus toledoi* sp. nov., *O. juquinha* and *Odontophrynus* sp. (aff. *juquinha*) comprise a clade with specimens distributed along three distinct mountain ranges in Brazil: Mantiqueira (*O. toledoi* sp. nov.) and Espinhaço (*O. juquinha*) mountains, both in southeastern Brazil, and Diamantina Plateau (*O.* aff. *juquinha*), in northeastern Brazil. The new species is morphologically similar and closely related to *O. juquinha*, but is distinguished in morphology (both adult and larval), karyotype (*O. toledoi* sp. nov. is tetraploid and *O. juquinha* is diploid), and corroborated by phylogenetic inferences. We also show that these species do not exchange haplotypes in the 16s gene. Furthermore, although the raw acoustic parameters of *Odontophrynus toledoi* sp. nov. and *O. juquinha* overlap at the limits of their ranges, we found a clear difference in the acoustic space structure.

Keywords. Atlantic Forest, burrowing toad, integrative taxonomy, species delimitation, species description.

Introduction

The genus *Odontophrynus* Reinhardt & Lütken, 1862 is composed by ground-burrowing medium-sized toads with nocturnal activity, distributed throughout eastern South America, from northeastern Brazil to southwestern Argentina, and mainly associated with open formations (Caramaschi & Napoli 2012; Frost 2021). The phylogenetic position of this genus and its species has been discussed for over a decade (Pyron & Wiens 2011; Martino *et al.* 2019; Magalhães *et al.* 2020). However, in spite of previous discussions, the genus could be phenotypically diagnosed by the putative synapomorphy of foot musculature (see Blotto *et al.* 2017). Currently, the genus includes ten species arranged in two species groups: the *O. americanus* and the *O. cultripes* groups, plus *O. occidentalis* (Berg, 1896), a species not associated to any group (Martino *et al.* 2019; Rosset *et al.* 2021).

The *Odontophrynus americanus* species group currently includes six species (Rosset *et al.* 2021): five diploid species with 2n = 22 chromosomes (*O. lavillai* Cei, 1985; *O. cordobae* Martino & Sinsch, 2002; *O. maisuma* Rosset, 2008; *O. juquinha* Rocha, Sena, Pezzuti, Leite, Svartman, Rosset, Baldo & Garcia, 2017; *O. reigi* Rosset, Fadel, Guimarães, Carvalho, Ceron, Pedrozo, Serejo, Souza, Baldo & Mângia, 2021); and *O. americanus* (Duméril & Bibron, 1841) as the only tetraploid species (2n = 4X = 44 chromosomes). The distribution of this group is known to central and eastern Argentina, southern Paraguay, Uruguay, and to Brazil, from the South to the central part of the state of Minas Gerais (Frost 2021). This group can be characterized by the absence of large dorsal tibial and forearm glands, and indistinctly developed postorbital, temporal, and parotoid glands, although glandular ridges may be present on postorbital and parotoid regions and on the posterolateral surface of the forearms (Savage & Cei 1965; Caramaschi & Napoli 2012).

One of the major taxonomic issues in this group is the identity of *O. americanus* throughout its geographic range. Several studies have pointed out the presence of more than one species under this name (Juncá *et al.* 2005; Martino *et al.* 2019; Rosset *et al.* 2021). In addition, there are populations with different ploidies referred to as *O. americanus* or *Odontophrynus* sp. (aff. *americanus*), and there are major gaps in the acoustic and genetic data, mainly from northern populations (see Rosset *et al.* 2006; Rocha *et al.* 2017; Martino *et al.* 2019). Thus, it is necessary to better evaluate these putative new cryptic taxa under the current name of *O. americanus*.

Integrative taxonomy is an important approach to understanding the identity and distribution pattern of species with the intersection of evidence from two or more independent lines of investigation (Padial *et al.* 2010). In anurans, polymorphic traits such as color patterns that are highly variable (Hoffman & Blouin 2000) may complicate the taxonomic identification of species. Herein lays the importance of combining multiple evidences of diagnostic traits. This is especially true for the genus *Odontophrynus*, for which there are several cryptic species (e.g., Rosset *et al.* 2006, 2021; Cianciarullo *et al.* 2019), and lack of genetic, acoustic, and larval data for several populations (see Rocha *et al.* 2017; Martino *et al.* 2019; Rosset *et al.* 2021).

The Brazilian Atlantic Forest comprises several types of phytophysiognomy from the Northeast to the Southern regions of the country; less than 10% of the original cover remains (Colombo & Joly 2010). The montane Atlantic Forest species diversity observed in the state of São Paulo has been attributed to factors such as the high structural complexity of the environments (Rossa-Feres *et al.* 2010). The highest lands in this region are in the Mantiqueira mountain range, which runs for about 900 km along the borders of the states of São Paulo, Rio de Janeiro, Espírito Santo, and Minas Gerais, in southeastern Brazil (Peixoto *et al.* 2020). The Mantiqueira mountain range harbors one of the most diverse anuran fauna in the Atlantic Forest and is considered a hotspot of anuran endemism (Silva *et al.* 2018; Muscat *et al.* 2020).

In the course of a survey of anurans in the highlands of the southern Mantiqueira mountains in the state of São Paulo, southeastern Brazil, we found a frog belonging to the *O. americanus* species group for which we found enough information (genetics, acoustics, osteology, larval and adult morphology) to consider it as a distinct species. During the course of our surveys in the district of São Francisco Xavier, municipality of São José dos Campos, state of São Paulo, we also gathered in-depth data of its natural history. Here is the description of the new species.

Material and methods

Specimens examined

We compared adult specimens with animals deposited in museums (Supp. file 1: specimens examined) and with data available in literature (e.g., Duméril & Bibron 1841; Cei 1985; Martino & Sinsch 2002; Rosset 2008; Rocha *et al.* 2017; Rosset *et al.* 2021).

Specimens used for comparisons are deposited in the following Brazilian collections:

CFBH	=	Célio F.B. Haddad amphibian collection, Universidade Estadual Paulista Júlio Mesquita Filho, Rio Claro, São Paulo
MNRJ	=	Museu Nacional, Universidade Federal do Rio do Janeiro
MZUSP	=	Museu de Zoologia, Universidade de São Paulo, São Paulo
MDBio	=	Museu de Diversidade Biológica (MDBio), Universidade Estadual de Campinas, São Paulo - Amphibian Collection (ZUEC-AMP), Video Collection (ZUEC-VID) and Sound Collection (FNJV)
CCLZU	=	Coleção Científica do Laboratório de Zoologia da Universidade de Taubaté, Taubaté, São Paulo

Morphology

We took 15 measurements with digital calipers (precision ± 0.01 mm): snout–vent length (SVL), head length (HL), head width (HW), internarial distance (IND), eye–nostril distance (END), eye diameter (ED), interorbital distance (IOD), thigh length (THL), tibia length (TbL), foot length (FL), and inner metatarsal tubercle length (IMT) following Watters *et al.* (2016); arm length (AL), hand length (HAL),

finger III length (F3L), and toe IV length (T4L), following Rosset *et al.* (2021). We followed Savage & Cei (1965) for parotoid, postorbital, and temporal glands anatomy and nomenclature. Terminology of the snout shape followed Heyer *et al.* (1990); webbing formula follows Savage & Heyer (1997). We determined which adults were males by checking the presence of vocal slits, vocal sacs, and nuptial pads on thumbs.

Tadpole description

Larvae external morphology was based on seven specimens between Gosner's (1960) stages 37–40. We took eight measurements following Altig & McDiarmid (1999): total length (TL); body length (BL); tail length (TAL); tail muscle width (TMW); interorbital distance (IOD); internarial distance (IND); maximum tail height (MTH); and tail muscle height (TMH). We followed Lavilla & Scrocchi (1986) for body height (BH); body width (BW); eye–snout distance (ESD); nostril–snout distance (NSD); eye–nostril distance (END); eye diameter (ED); nare diameter (ND); and snout–spiracular distance (SSD). For dorsal fin height (DFH); ventral fin height (VFH); and for oral disc width (ODW) we followed Grosjean (2005). In the labial tooth row formula (LTRF): A-1 (first anterior labial tooth row) and A-2 (second anterior labial tooth row) refers to anterior portion of labial tooth; P-1(first posterior labial tooth row), P-2(second posterior labial tooth row), and P-3 refer (third posterior labial tooth row) to posterior portion of labial tooth. We followed Pinheiro *et al.* (2012) for spiracle length (SL). Spiracle width (SW) measurements were also taken. We took all linear measures to the nearest 5 mm using software TPSDig2 (Rohlf 2015, 2017). ND, SL and SW were taken using stereo microscope Zeiss Discovery V. 20 to the nearest 0.5 mm. Lateral line system was described based on Lannoo (1987).

To compare morphology between tadpoles of the genus *Odontophrynus*, we performed principal component analysis (PCA) by building a comparative table of the species of the genus *Odontophrynus* with the same 21 measurements (Supp. file 1: Table S2) used in description of the tadpole *O. toledoi* sp. nov. The comparative table was built using information present in literature and we inferred measurements from the pictures and illustrations using TPSDig2 (Rohlf 2017). We used means of the morphological measurements provided by authors or maximum range when measurements were inferred from the illustrations. We have three main measurements present for all descriptions of tadpoles: total length (TL), body length (BL), and tail length (TAL). However, some measurements were not present in all tadpole descriptions. We had 30.5% missing data concentrated in additional measurements (e.g., ESD, NSD, END, SSD, SL, SW), but 69.5% of the most common measurements were present. For this, we used an imputation method by cross-validation, which led to the smallest mean square error of prediction to estimate the number of dimensions for the PCA using the estim_ncpPCA function of the missMDA package (Josse & Husson 2016). Also, we used imputePCA of the missMDA package (Josse & Husson 2016) to estimate the missing values based on the number of components estimated previously. All analyses were performed in R software ver. 4.1.3 (R Core Team 2022).

Osteology

We analyzed six specimens from São Francisco Xavier, São José dos Campos, São Paulo, Brazil (ZUEC-AMP 24833 [holotype], 24718, 24725, 24831, 24832, and 24834), housed in the amphibian collection of the MDBio, at the Universidade Estadual de Campinas (Unicamp), Campinas, Brazil. We ran microtomography to avoid the destruction of type series. The images were taken by a Skyscan-1173 Bruker® microtomograph at source voltage (kV) 47, source current (uA) 154, depth (bits) 16, exposure (ms) 560, and rotation step (deg) 0.180. We used the DataViewer and CTVox softwares (licensed by Bruker®) to analyze 3D images and to perform the measurements. We produced two 3D videos of the holotype (ZUEC-AMP 24833) and a paratype (ZUEC-AMP 24725) to show osteological structures, deposited in the video collection of the MDBio (ZUEC-VID 969 and 970, respectively). We also cleared and stained one specimen of the new species from Inconfidentes, Minas Gerais (ZUEC-AMP 23469), to observe some structures that weren't defined in the microtomography. We took the following

measurements from the tomographed individuals: mandible to ischium length (MIL), skull width (SKW), skull length (SKL), width of frontoparietal (WFP), length of vertebra II (LV2), length of sacral vertebra (LSV), sacral diapophyses width (SDW), SKW/MIL, SKL/MIL, SKW/SKL, LV2/MIL, and LSV/MIL. Osteological description and terminology are based on Lynch (1971), Trueb (1977), and Duellman & Trueb (1994).

Bioacoustics

We analyzed 100 calls from 15 adult males of *Odontophrynus toledoi* sp. nov. (Parque Estadual de Campos do Jordão, SP, n = 3; 32 notes/calls; Santo Antônio do Pinhal, SP, n = 2; 12 notes/calls; São Francisco Xavier, São José dos Campos, SP, n = 10; 56 notes/calls). Recordings are housed at Fonoteca Neotropical Jacques Vielliard (FNJV), in the Museu de Diversidade Biológica (MDBio), of Universidade de Campinas (UNICAMP) under the numbers FNJV 50453–67. For the analyses we used a call-centered approach (see Köhler *et al.* 2017).

We performed the bioacoustics analyses using Raven Pro ver. 1.6 (Bioacoustics Research Program 2019) with Hann window type, 512 samples, 3 dB filter bandwidth 61.9 Hz, overlap of 50%, hop size 256 samples, DFT size 512 samples, and grid spacing 43.1 Hz. We analyzed eight different traits: frequency range (minimum frequency and maximum frequency), dominant frequency (the region with the highest energy, obtained with the 'peak frequency' function and power spectrum), note duration, number of pulses, pulse duration, pulse interval, and pulse rate. The terminologies used for the vocalization parameters are in agreement with Martins & Jim (2003) and Köhler *et al.* (2017).

Currently, multivariate analyses that explore acoustic-space have become increasingly common for the diagnosis of cryptic species (e.g., MacLeod *et al.* 2013; Andrade *et al.* 2020). In this approach, spectrograms are compared by using a variant of eigensurface analysis to sample and compare these surfaces (MacLeod *et al.* 2013). The SoundShape package (Rocha & Romano 2021) in R software implements the geometric morphometric approach to compare the acoustic-space of species. SoundShape first applies a 3D sampling grid to the spectrogram, which allows the extraction of coordinates (semilandmarks) that correspond to the acoustic attributes of the species and how they are distributed in the acoustic-space. These positions are later used in a principal coordinate analysis (PCA) that summarizes the acoustic information, allowing for the comparison of different species. For this reason, and since the acoustic parameters of closely related species can phylogenetically overlap, we used this approach to explore the acoustic-space of *Odontophrynus toledoi* sp. nov. and *Odontophrynus juquinha*. These species possibly have similar calls and parameters that overlap in range. Although PCA is not a hypothesis test per se, it allows visualization of the variation of acoustic attributes along fewer axes than when looking at the original dataset.

Karyotype

We obtained chromosomes from intestinal epithelium and testicular cell suspensions of five males, all collected in Santo Antônio do Pinhal, SP, Brazil. Specimens were deposited at the MDBio, Unicamp (ZUEC-AMP 24763 to 24767). We anesthetized the individuals (lidocaine 50 mg/g – cutaneous administration) after pre-treatment in vivo with colchicine 2% (0.02 ml/g body weight) for 4 h. We obtained chromosome preparations according to King & Rofe (1976), with modifications from Gatto *et al.* (2018), and Schmid *et al.* (1979). We stained the chromosomes with Giemsa (10%), C-banded (King 1980), and silver-impregnated using the Ag-NOR method (Howell & Black 1980).

Phylogenetic inference

We sequenced fragments of the 16S ribosomal RNA mitochondrial gene of 19 individuals from the new species and 18 from other species of *Odontophrynus*; we also included sequences of nine

species of *Odontophrynus* available in GenBank (Supp. file 1: Table S1). All localities are listed in Supp. file 1: Table S1.

We extracted DNA from ethanol-preserved tissues from either liver or muscle, using an ammonium acetate precipitation method (adapted by Lyra *et al.* 2017) and DNeasy Blood & Tissue kit (QIAGEN Inc.) following the manufacturer's guidelines. We used the An16SF and An16SR primer pair designed by Lyra *et al.* (2017) following polymerase chain reaction (PCR) conditions described by the same authors. We purified PCR products using a mix of 0.5 unit of thermosensitive alkaline phosphatase (FastAP) and 1 unit of Exonuclease I (Thermo Fisher Scientific Inc.) diluted in 2.45 lL of ultrapure water per PCR, incubated for 30 min at 37°C followed by 5 min at 95°C. We sequenced the purified PCR products with BigDye Terminator Cycle Sequencing Kit (ver. 3.0, Applied Biosystems) in an ABI 3730 automated DNA sequencer (Applied Biosystems) at Centro de Biologia Molecular e Engenharia Genética, Unicamp, Campinas, SP, Brazil.

We edited and aligned the resulting sequences in Geneious ver. 9.1.2 with the MUSCLE algorithm using default parameters (Edgar 2004). We found gaps in 16S and to avoid possible bias we removed it using Gblocks (Talavera & Castresana 2007). The final dataset was 347 base pairs (bp; 92% of the original 375 positions). We deposited all sequences in GenBank (Supp. file 1: Table S1).

We used IQ-TREE ver. 2.1.3 (Nguyen *et al.* 2015) to infer a maximum likelihood (ML) gene tree of the 16S mtDNA dataset. We used ModelFinder (Kalyaanamoorthy *et al.* 2017) to select the best-fit substitution model using the Bayesian Information Criterion (BIC), and the best-fit model was TN+F+G4. Support for nodes was assessed using both SH-aLRT with 1000 replicates (Guindon *et al.* 2010) and UFBoot with 10 000 replicates (Hoang *et al.* 2018). All phylogenetic analyses in this study were rooted using *Proceratophrys appendiculata* (Günther, 1873) and *P. boiei* (Wied-Neuwied, 1824) as outgroups.

We used BEAST ver. 2.6.5 (Bouckaert *et al.* 2019) to estimate a gene tree using Bayesian inference with the same 75 sequences used in IQ-TREE analysis. We employed a relaxed clock exponential and bModelTest for model selection (Bouckaert & Drummond 2017) and a constant size coalescent tree prior. We ran the analysis for 50 million generations, sampling every 2000 steps. We checked for stationarity by visually inspecting trace plots and ensuring that all values for effective sample size (ESS) were above 200 in Tracer ver. 5 (Drummond & Rambaut 2007). The first 10% of sampled genealogies were discarded as burn-in, and we calculated the maximum clade credibility tree with median node ages with TreeAnnotator ver. 1.8 (Drummond *et al.* 2012).

Based on our single loci (16S) data, to retrieve the evolutionary mitochondrial lineages, we implemented tree-based methods used for species delimitation. We used the BEAST generated tree in a Bayesian implementation of the Generalized Coalescent Yule (bGMYC) model with the bGMYC package (Reid & Carstens 2012), in R software (R Core Team 2022). The GMYC method performs a model-based analysis to locate threshold points (or nodes) in the genealogy where there are transitions in branching rates, reflecting inter- or intra-specific evolutionary processes (Pons *et al.* 2006). We also employed a Bayesian Phylogenetics and Phylogeography (BPP) analysis as a complementary method. BPP is a Monte Carlo Markov Chain (MCMC) program that analyzes DNA sequence alignments under the multispecies coalescent model (MSC) (Rannala & Yang 2003).

In order to explore the relationship among haplotypes, we estimated haplotype networks among *Odontophrynus* spp. for the recovered clade in the Bayesian topology, in POPART software (Leigh & Bryant 2015) using median-joining network method.

Results

<div align="center">

Class Amphibia Linnaeus, 1758
Order Anura Fischer Von Waldheim, 1813
Family Odontophrynidae Lynch, 1969
Genus *Odontophrynus* Reinhardt & Lütken, 1862

***Odontophrynus toledoi* sp. nov.**
urn:lsid:zoobank.org:act:E7AE4CE9-728E-438A-AF75-8C6EC6C84306
Figs 1–2

</div>

Odontophrynus americanus – Savage & Cei 1965. — Beçak *et al.* 1966. — Araújo *et al.* 2009. — Lyra *et al.* 2017.
O. aff. *americanus* 1 – Martino *et al.* 2019.
Odontophrynus aff. a*mericanus* – Rosset *et al.* 2021.

Diagnosis

Odontophrynus toledoi sp. nov. is a medium-sized species belonging to the genus *Odontophrynus* based on the phylogenetic position and a combination of morphological characters: granular skin on the dorsum and venter, head wider than long, snout truncate in profile, tympanum hidden, first subarticular tubercle on toe I enlarged, inner metatarsal tubercle large, tarsal fold short (Savage & Cei 1965; Caramaschi & Napoli 2012). The new species belongs to the *Odontophrynus americanus* species group based on phylogenetic affinities and the combination of the following characters: absence of large dorsal, tibia and forearm glandular warts, with postorbital, temporal, and parotoid glandular warts not distinctly developed but with a series of small glandular warts of irregular size and shape, forming glandular ridges longitudinally oriented, on postorbital-parotoid regions (Caramaschi & Napoli 2012). *Odontophrynus toledoi* is distinguished from the remaining species belonging to the *O. americanus* group by the following combination of characters: (1) medium sized (SVL = 40.4–51.8 mm in males and 45.0–54.5 mm in females of *O. toledoi*; Table 1); (2) head wider than long (HW/HL = 1.31); (3) dorsal surface of head, arms, body and limbs dark brown with arms and limbs with light brown stripes; (4) light mid-dorsal stripe present or interrupted in most of the specimens; (5) yellowish stripe between the eyes, resembling a ')' shape; (6) increased number of longitudinally oriented dorsal glandular ridges; (7) karyotype with $2n = 4X = 44$, with fundamental number = 88; (8) advertisement call with dominant frequency of 775–1033 Hz; (9) pulse rate of 89–132 pulses/s; (10) large tadpoles (mean TL = 42.91–56.18 mm); (11) one–two submarginal papillae on the posterior labium of each side of the oral disc near the posterior emargination; and (12) spiracle sinistral, short, inner wall fused to the body with small distal portion free.

Etymology

The specific epithet honors Professor Luís Felipe Toledo for his contribution in solving the mysteries of the natural history of Neotropical amphibians, especially those from southeastern Brazil and mostly within the Atlantic Forest, where the new species resides.

Type material

Holotype

BRAZIL • adult ♂, SVL 49.3 mm; São Paulo State, São José dos Campos, São Francisco Xavier, collected at Rio Manso; 22°54′05″ S, 45°52′43″ W; 1042 m a.s.l.; datum WGS-84; 1 Jan. 2020; E. Muscat and M.T. Moroti leg.; ZUEC-AMP 24833.

Paratypes

BRAZIL – **São Paulo State** • 1 adult ♀; São José dos Campos, São Francisco Xavier, collected at Projeto Dacnis private reserve; 22°53′45.81″ S, 45°56′30.46″ W; 751 m a.s.l.; datum WGS-84; 15 Jan. 2019; E. Muscat leg.; ZUEC-AMP 24641 • 1 adult ♀; same locality as for holotype; 21 Jul. 2019; E. Muscat and D. Stuginski leg.; ZUEC-AMP 24725 • 2 adult ♀♀; same locality as for holotype; E. Muscat and M.T. Moroti leg.; ZUEC-AMP 24831 • 2 adult ♂♂; same collection data as for preceding; ZUEC-AMP 24834 • 5 adult ♂♂; Santo Antônio do Pinhal; collected at RPPN Fazenda Renópolis; 22°48′20.93″ S, 45°37′32.96″ W; 1332 m a.s.l.; datum WGS-84; 21 Aug. 2019; N.J.S. Fernandes and I.A. Martins leg.; ZUEC-AMP 24763 to 24767.

Non-type material examined

BRAZIL – **São Paulo State** • 1 adult ♀; Campos do Jordão, collected at Parque Estadual Campos do Jordão (Horto Florestal); 22°39′55.1″ S, 45°26′59.9″ W, 1531 m a.s.l.; WGS-84; 26 Oct. 2005; I.A. Martins, P.H. Bernardo, F.B.R. Gomes and A.P. Suarez leg.; CCLZU 175 • 2 adult ♂♂; Campos do Jordão, collected at Parque Estadual Campos do Jordão (Horto Florestal); 22°39′55.2″ S, 45°27′12.7″ W; 1520 m a.s.l.; WGS-84; 26 Oct. 2005; I.A. Martins, P.H. Bernardo, F.B.R. Gomes and A.P. Suarez leg.; CCLZU 181-182 • 3 adult ♂♂; Campos do Jordão, collected at Parque Estadual Campos do Jordão (Horto Florestal); 22°41′55.2″ S, 45°27′12.7″ W; 1711 m a.s.l.; WGS-84; 17 Jan. 2005; I.A. Martins, F.B.R. Gomes and A.F. Leite leg.; CCLZU 1484 to 1486 • 1 adult ♀; Campos do Jordão, Parque Estadual de Campos do Jordão (Horto Florestal); 7 Dec. 2009; I.A. Martins, F.B.R. Gomes, C.R. Silva and V.A. Mendes leg.; CCLZU 2637 • 1 adult ♂; same collection data as for preceding; CCLZU 2638. – **Minas Gerais State** • 1 adult ♂; Itamonte; 22°16′58.85″ S, 44°52′11.56″ W; 905 m a.s.l.; WGS-84; 7 Sep. 2004; I.A. Martins leg.; CCLZU 1487 • 1 adult ♀; Cristina, collected at Mata da Prefeitura; 22°13′05″ S, 45°15′25″ W; 1150 m a.s.l.; WGS-84; 25 Aug. 2005; A.F.B Junqueira leg.; CCLZU 2040 • 1 adult ♂; Cristina, collected at Mata da Prefeitura; 25 Aug. 2005; A.F.B Junqueira leg.; CCLZU 2023 • 1 adult ♀; Maria da Fé; 22°18′15.5″ S, 45°22′43.2″ W; 1265 m a.s.l.; WGS-84; 15 Sep. 2007; A.F.B. Junqueira and F.B.R. Gomes leg.; CCLZU 2525 • 1 adult ♂; Maria da Fé; A.F.B. Junqueira and F.B.R. Gomes leg.; CCLZU 2526 • 2 adult ♀♀; Marmelópolis; 22°30′31.9″ S, 45°09′00″ W; 1570 m a.s.l.; datum WGS-84; 24 Sep. 2009; I.A. Martins leg.; CCLZU 2918, 2919 • 1 adult ♀; Marmelópolis; 13 Nov. 2009; I.A. Martins leg.; CCLZU 2964 • 1 adult ♂; Marmelópolis; 22 Jan. 2010; I.A. Martins leg.; CCLZU 3015 • 1 adult ♀; Inconfidentes; 27 May 2014; Souza J. leg.; ZUEC-AMP 23469.

Description of the holotype

Adult male, body stout, SVL 49.3 mm (Fig. 1, Table 1). Head wider than long (HW 41.1% of SVL, HL 33.2% of SVL, HW/HL = 1.23). Snout rounded in dorsal view and truncate in lateral view. Canthus rostralis slightly distinct, concave in dorsal view. Loreal region slightly concave. Nostrils elliptic elongated, directed dorsolaterally, and situated at the tip of the snout in lateral view. Internarial distance smaller than eye to nostril distance (IND 71.4% of END) and smaller than interorbital distance (IND 31.2% of IOD). Eyes large, prominent and laterally oriented (ED 32.3% of HL). Upper eyelid with one elongated glandular wart and with a glandular ridge along its marginal edge. Tongue rounded, approximately half free and notched posteriorly. Vomerine teeth in two patches between and the in same line of the choanae. Vocal slits present, longitudinal. Vocal sac well developed, median, subgular. Tympanum hidden, not visible externally. Dorsum of head, body, and limbs with scattered distributed glandular warts, more abundant in flanks. Anterior half of dorsum with series of distinct elongated glandular warts with irregular size and shape, forming small discontinuous pairs of ridges longitudinally oriented behind the postorbital region, parotoid region and in the interscapular region. Skin of venter uniformly covered with small and rounded glandular warts. Forelimbs stout (AL 50% of SVL) covered with small glandular warts, except on dorsal surface of fingers. Ventrolateral surface of forearms with longitudinal series of two elongated glandular warts, fused into ridge. Fingers slender with rounded

Table 1. Measurements (in mm) of the holotype and 10 paratypes of *Odontophrynus toledoi* sp. nov. The results are presented as the mean ± standard deviation (sd) and minimum–maximum values (range). Abbreviations of morphometric characters are defined in Material and methods.

Morphometric characters	Holotype	Male (n = 6)		Female (n = 4)	
		Mean ± sd	Range	Mean ± sd	Range
SVL	49.3	45.6 ± 4.1	(40.4–51.8)	51.5 ± 4.5	(45.0–54.5)
HL	16.4	14.4 ± 1.3	(13.0–16.7)	16.3 ± 1.2	(15.0–17.9)
HW	20.3	18.8 ± 1.3	(17.6–20.5)	22.0 ± 0.9	(21.2–23.1)
END	3.5	3.4 ± 0.6	(3.0–4.5)	3.7 ± 0.8	(2.9–4.6)
IND	2.5	2.5 ± 0.3	(2.0–2.9)	3.0 ± 0.4	(2.6–3.5)
ED	5.3	4.8 ± 0.6	(3.9–5.4)	5.5 ± 0.6	(5.0–6.3)
IOD	8.0	6.8 ± 0.6	(5.9–7.8)	8.1 ± 0.8	(7.1–8.9)
AL	25.0	22.6 ± 1.7	(19.9–24.7)	25.0 ± 2.2	(21.8–26.3)
HAL	15.5	13.7 ± 1.0	(12.2–14.7)	15.0 ± 1.6	(12.6–16.3)
F3L	4.8	4.3 ± 0.3	(3.9–4.9)	5.0 ± 0.5	(4.5–5.5)
THL	17.9	17.6 ± 1.4	(15.1–19.1)	19.2 ± 2.4	(16.2–22.0)
TbL	16.7	14.8 ± 1.2	(13.2–16.2)	17.4 ± 1.2	(16.0–18.8)
FL	23.8	21.2 ± 1.3	(19.9–23.5)	24.2 ± 1.9	(22.5–26.8)
T4L	11.8	10.3 ± 0.6	(9.4–11.1)	11.9 ± 0.4	(11.6–12.6)
IMT	4.6	4.1 ± 0.6	(3.5–5.1)	4.9 ± 0.5	(4.4–5.6)

tips; dermal fringes absent; interdigital webbing absent. Length of fingers: IV>II>V≥III. Subarticular tubercles large, nearly bilobated, proximal more developed than distal. Supernumerary tubercles rounded to oval, covering the palmar surface. Nuptial pads present on thumbs and posterior surface of inner metacarpal tubercles. Inner and outer metacarpal tubercles large, inner oval and outer longitudinally divided, internal part oval, external part elongated. Nuptial pads present on thumbs and posterior surface of inner metacarpal tubercles. Hind limbs stout and relatively short. Tarsal fold present, slightly curved, as long as inner metatarsal tubercle and approximately same length as tarsus. Toes slender with rounded tips; dermal fringes slightly developed; interdigital webbing present. Lengths of toes: IV>III≥V>II>I. Webbing formula: I 1–2 II 1–3 III 2–4 IV 4–2 V. Inner metatarsal tubercle large (IMT 19.3% of FL), shovel-like, with external border keratinized; outer metatarsal tubercle slightly distinct; subarticular tubercles rounded, subarticular tubercle of toe I and II, enlarged, greater than others. Supernumerary tubercles small and rounded, aligned, and covering the plantar surface.

Coloration of the holotype in life

Dorsal surface of head, arms, body, and limbs dark brown (Fig. 2). Arms and limbs with light brown blotches resembling stripes over a dark brown background. A horizontal yellowish stripe between the eyes, resembling a ')' shape. Yellowish dorsolateral stripes, starting behind the head towards the hind limbs. A yellow interrupted mid-dorsal stripe. Irregularly sized light and dark brown blotches distributed below the dorsolateral yellowish stripe. Upper lip yellowish interrupted by dark brown blotches. Vocal sac moss green to black. Venter whitish scattered with grey blotches gradually increasing on the side of the body. Nuptial pads light brown. Foot with outer metatarsal, subarticular, and supernumerary tubercles gray over light brown background. Tarsal fold grayish. Inner metatarsal tubercle light brown

with keratinized dark brown portion. Iris with three marbled colors: golden in the dorsal region, black in the middle and whitish in ventral region; pupil horizontally elliptical with golden margins.

Coloration of the holotype in preservative

Dorsal background color predominantly dark brown. Light brown blotches on the arms and limbs. The yellowish stripes became light brown; the whitish or grayish coloration of the antebrachial glandular wart, tubercles of the hand and foot, and tarsal fold became cream-colored. Venter yellowish-colored, with scattered dark brown blotches gradually increasing on the sides of the body. Gular area with dark grey pigmentation.

Variation of adult specimens

Males of *O. toledoi* sp. nov. differ from females by the presence of a black pigmented gular region on the vocal sac, and well-developed nuptial pads on thumb and posterior surface of inner metacarpal tubercles. Adult females are usually bigger than adult males. Longitudinally oriented glandular warts and the light brown blotches varied in number, size, and shape among individuals. The ')' stripe between the eyes can
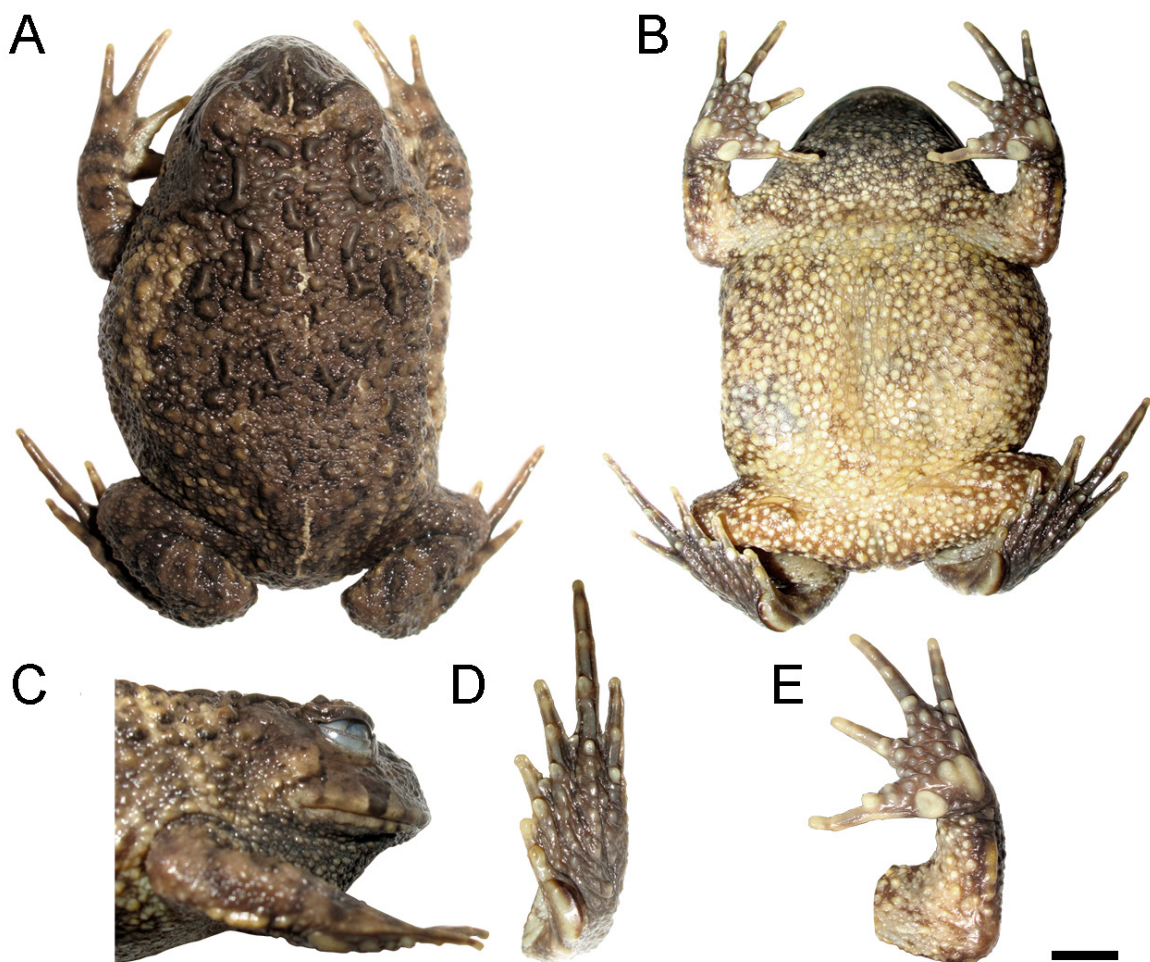

Fig. 1. *Odontophrynus toledoi* sp. nov., holotype, ♂ (ZUEC-AMP 24833). **A**. Dorsal view. **B**. Ventral view. **C**. Lateral view of the head. **D**. Ventral view of the foot. **E**. Ventral view of the hand. Scale bar = 5 mm.

be poorly distinguished in some individuals and one individual had a distortion, interrupting the stripe. Mid-dorsal stripe is discontinuous and can begin on the head or not.

Tadpoles

Larvae external morphology

Tadpoles of *Odontophrynus toledoi* sp. nov. have a total length of 42.91–56.18 mm (47.71 ± 5.34 mm) in Gosner stages 37–40 (Lot ZUFMS-AMP 15276, Fig. 3, Table 2). Body is depressed (BH/BW = 0.85–0.86; Fig. 3A–C), rounded in lateral view (BL/BH = 1.81–1.86), elliptical in dorsal view (BL/BW = 1.55–1.58), and slightly longer than one third of the total length (BL/TL = 0.36–0.37). Snout is rounded in lateral view and ovoid in dorsal view. Eyes dorsal, dorsolaterally oriented. Nostrils dorsal with oval shape, anterolaterally positioned with an elevated marginal rim, undeveloped inner margin projection, and closer to the tip of the snout than the eye (NSD/END = 0.77–0.79; Fig. 3G). Spiracle sinistral, short, inner wall fused to the body with small distal portion free, lateroventrally positioned, posterodorsally directed, and placed at half of the body length (SSD/BL = 0.57–0.60; Fig. 3F). Ventral tube median, dextral opening, ventrally directed, fused to the ventral fin with posterior portion free and positioned slightly below ventral margin (Fig. 3D–E). The dorsal membrane of the ventral tube is slightly shorter than the ventral membrane (Fig. 3D). Intestinal mass is circular, located at the center and slightly displaced to the left from the abdomen (Fig. 3C). Tail has acute tip, comprising 62.3% of the total length and higher than the body (MTH/BH = 1.02–1.06). Tail musculature is slightly developed (TMH/BH = 0.46–0.51), myotomes visible and more developed on the anterior third and mid portion, and reach the tip of the tail. Dorsal fin has slightly more convex margin than the ventral fin. Dorsal fin high (DFH/TMH = 0.83–1.00) and ventral fin high (VFH/TMH = 0.52–0.60) with maximum height at the mid of the tail. Dorsal fin emerges at the posterior third of body, and the origin of ventral fin is at the inferior margin of ventral tube. Lateral line system has four neuromasts, almost indistinguishable, accumulated near the ventral tube, and others that we could delimit as: supraorbital around the eyes (SO); infraorbital around the snout and nares (IO); posterior supraorbital (PSO); posterior infraorbital near the musculature insertion (PIO); dorsal near the middle of tail musculature (D); and middle (M) on the half of body side (Fig. 3H– I).
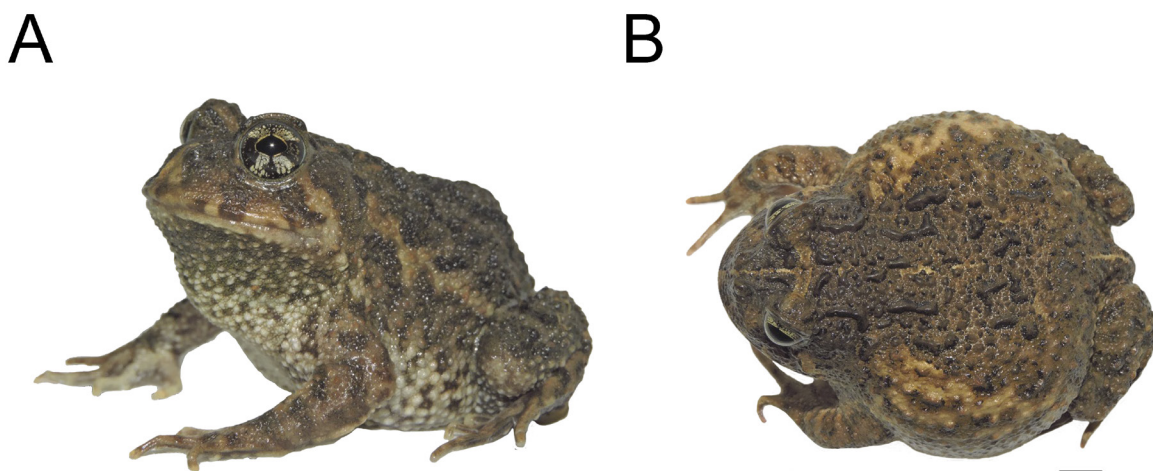

Fig. 2. *Odontophrynus toledoi* sp. nov., holotype, ♂ (ZUEC-AMP 24833), in life. **A**. Lateral view. **B**. Dorsal view. Scale bar = 5 mm.
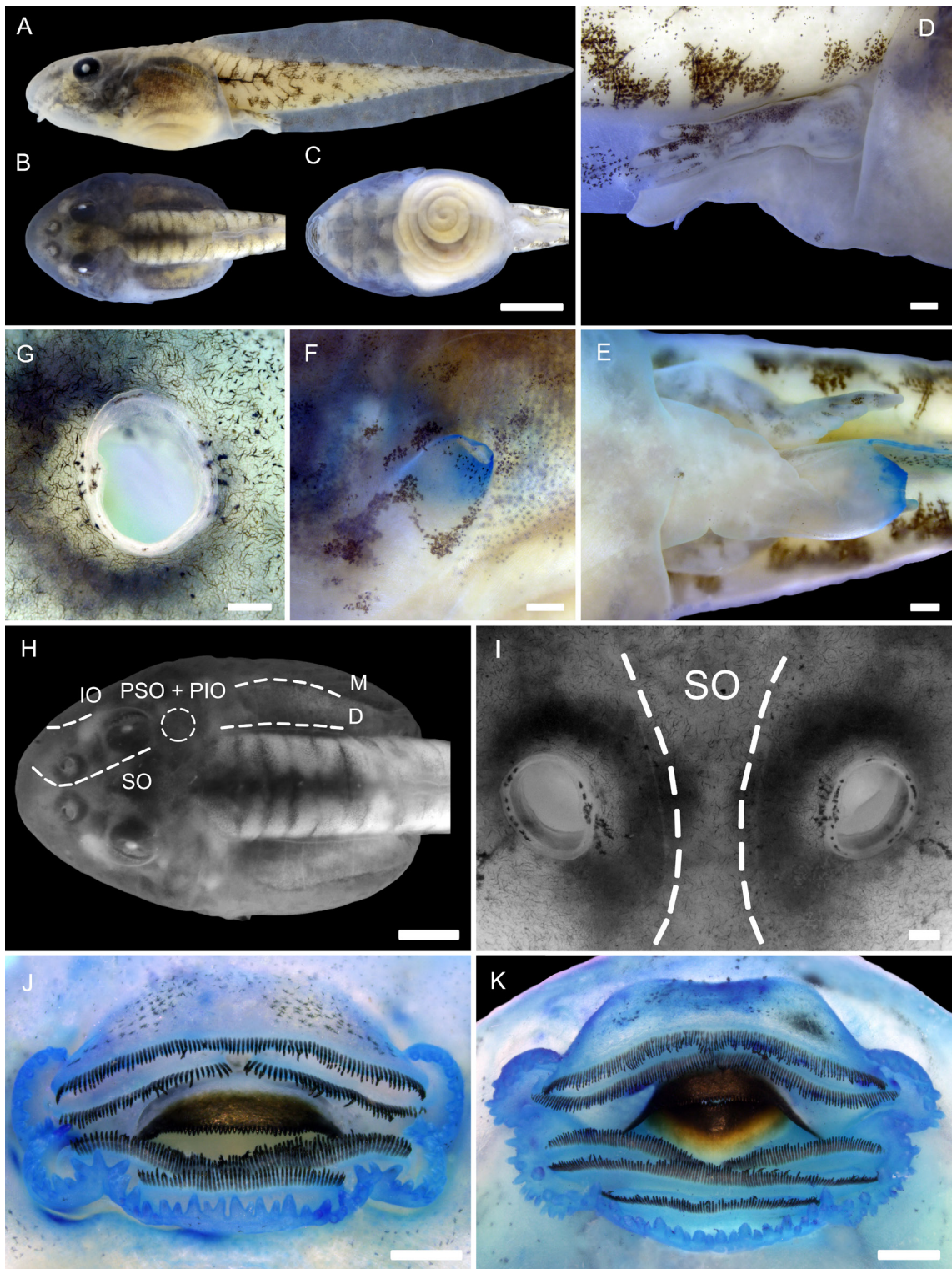
Fig. 3. *Odontophrynus toledoi* sp. nov., external morphology of the tadpole at stage 37–40. **A–C.** Lateral (A), dorsal (B), and ventral (C) views. **D–E.** Ventral tube. **F.** Spiracular aperture. **G.** Keft nare with an elevated marginal rim. **H–I.** Body on dorsal view and front view respectively indicating visible series of the lateral line system: supraorbital (SO), infraorbital (IO), posterior supraorbital (PSO), posterior infraorbital (PIO), dorsal (D), and middle (M). **J.** Oral disc closed. **K.** Oral disc opened. Scale bars: A–C = 5 mm; D–F = 0.5 mm; G = 0.2 mm; H = 2.5 mm; I = 0.2 mm; J–K = 0.5 mm.

Table 2. Tadpole measurements of *Odontophrynus toledoi* sp. nov. between Gosner stages 37 and 40 (n = 7). Data are in millimeters and presented as mean ± sd. *sd = standard deviation. For abbreviations see material and methods.

Measurements	Mean ± sd	Range
TL	47.71 ± 5.34	42.91–56.18
BL	17.95 ± 1.97	15.76–20.65
TAL	29.76 ± 3.42	26.81–35.53
BH	9.79 ± 1.13	8.48–11.41
BW	11.10 ± 1.28	9.95–13.28
MTH	10.32 ± 1.19	8.69–12.10
TMH	4.69 ± 0.48	4.39–5.20
DFH	4.34 ± 0.51	3.68–5.20
VFH	2.60 ± 0.28	2.32–3.14
TMW	4.30 ± 0.40	3.79–5.07
IOD	5.41 ± 0.48	4.91–6.01
IND	2.27 ± 0.17	2.11–2.58
ESD	5.66 ± 0.49	5.23–6.46
NSD	2.50 ± 0.26	2.25–2.87
END	3.16 ± 0.27	2.90–3.59
ED	2.26 ± 0.18	2.00–2.48
ND	0.64 ± 0.07	0.51–0.69
SSD	10.70 ± 0.99	9.58–11.84
SL	2.30 ± 0.57	1.44–3.12
SW	0.62 ± 0.08	0.49–0.72
ODW	3.46 ± 0.42	2.93–4.05

Oral disc small (ODW/BW = 0.29–0.30) anteroventrally positioned, laterally and posteriorly emarginated (Fig. 3A, J–K). Anterior labium has one single row of laterally long marginal papillae aligned on the top and alternated near the emargination with a wide gap anteriorly equivalent to P-2. Papillae aligned, reduced and spaced in lateral emargination. Posterior labium has one single row of long marginal papillae alternated without pigmentation and some bifid aligned papillae, about 14 papillae/mm with four bifid papillae (estimated on the posterior labium; Fig. 3J). There are one–two submarginal papillae on the posterior labium of each side of the oral disc near the posterior emargination. Submarginal papillae may be absent or not visible during initial stages (e.g., 30–37; Gosner 1960). Labial tooth row formula (LTRF) is 2(2)/3(1) with a short gap in A-2 and P-1; A-1 slightly shorter than A-2; P-1 and P-2 have the same size, both longer than P-3 (Fig. 3J–K). Labial teeth dark-colored arranged in a single row, one per tooth ridge with variable size. There are about 52 labial teeth/mm (estimated on P-3). Jaw sheaths serrated, heavily keratinized (with about 37 serrations/mm), and dark with lower sheath base ranging from brown to dark yellow. Upper jaw is arc-shaped with long lateral projection and lower sheath V-shaped, with lower jaw sheath slightly wider than the upper one (Fig. 3K).

Coloration of tadpoles in life

Body greenish in life with scattered dark blotches distributed all over it and concentrated on the lateral view of the body. Ventral region cream. Tail light cream with dark blotches, with concentration on last third of the tail. Musculature of the caudal portion easily seen due its reddish coloration (Fig. 4A). Mid dorsal cream stripe present in imagoes dorsum (Fig. 4B).

Coloration of tadpoles in preservative

Body coloration in preservative 10% formalin is light yellow or cream on the lateral view and dark yellow on dorsal view with melanophores located mainly near the eyes, nares, and on the anterior insertion of tail musculature on dorsal view. There are some angular patches on tail musculature and dorsal and ventral fins on the lateral view. Fins translucent with iridophores, mainly on the dorsal fin. The intestinal region is translucent with small melanophores near to oral disk.

Osteology

Odontophrynus toledoi sp. nov. has a semicircular shaped skull (Figs 5–6), wider than long (SKW/SKL = 1.41 ± 0.19; Table 3) and more elevated posteriorly. Frontoparietal relatively large, broad (width of frontoparietal 5.04 mm ± 0.59 mm), anterior margin rounded, posterior margin crescent-shaped, in contact medially without exposing frontoparietal fontanelle. Nasals triangular, wider than long, keeled, slightly separated from one another medially and well separated from the frontoparietal posteromedially; maxillary process of the nasals in contact with the pars facialis of the maxilla, and with the nasal process of the pterygoids. Maxillary arch complete. Short and wide alary process of the premaxilla. Pars facialis of maxillae bearing around 32 teeth, pars palatina broad, pterygoid process well developed, reaching the level of quadratojugal, wide anterior portion oriented to nasal and posterior portion that contacts maxillary process of nasals. Quadratojugals well developed, contacting maxilla. Vomers moderately sized, separated medially, prechoanal, postchoanal and anterior processes of the vomer well developed, anterior process contacts maxillary arch, dentigerous process of vomer bearing 4–5 teeth. Parasphenoid triradiate, cultriforme process pointed with four peaks, alae perpendicular to cultriform process. Zigomatic ramus of the squamosal moderately sized, anteroventrally directed, separated from the maxilla, enlarged posteriorly and rounded at the anterior end; otic ramus longer than zygomatic ramus. Sphenethmoid well developed, extending anteriorly to the anterior margin of the nasals. Palatines large, strong, narrowly separated medially, expanded laterally. Pterygoides triradiate, relatively large; anterior ramus long connected with maxilla, extending anteriorly to palatine, dorsally curved reaching maxillary process of nasals; medial ramus in contact with otic capsule. Prootic and exoccipital well developed. Occipital condyles large and broadly separated. Crista parotica broad and quadrangular. Posteromedial hyoid process long and well ossified. Vertebral column with 8 presacral vertebrae, I and II imbricate;
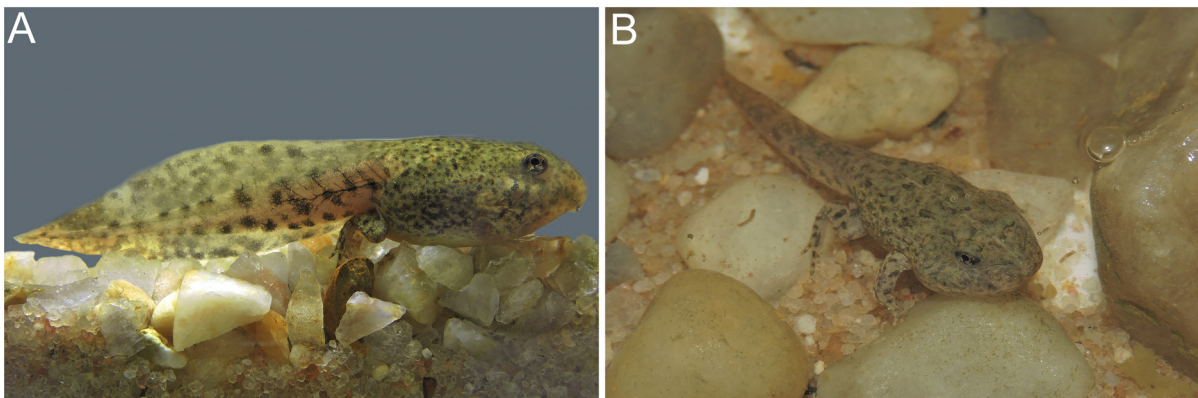

Fig. 4. *Odontophrynus toledoi* sp. nov. in life. **A**. Tadpole. **B**. Metamorph.
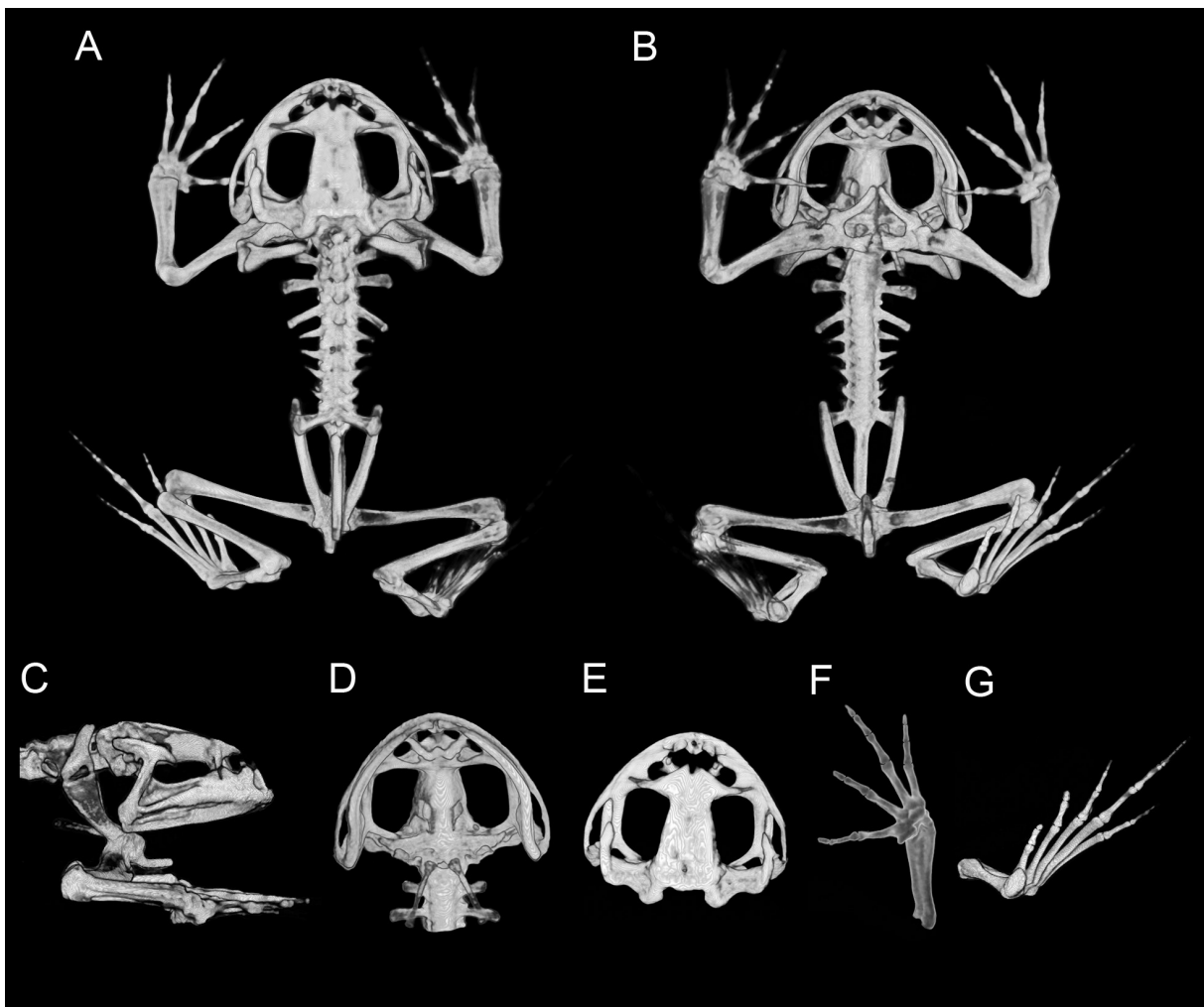
Fig. 5. *Odontophrynus toledoi* sp. nov., holotype, ♂ (ZUEC-AMP 24833), skeleton, generated by microtomography. **A**. Dorsal view of the individual. **B**. Ventral view of the individual. **C**. Lateral view of the head and arms. **D**. Ventral view of the skull. **E**. Dorsal view of the skull. **F**. Ventral view of the hand. **G**. Ventral view of the foot.
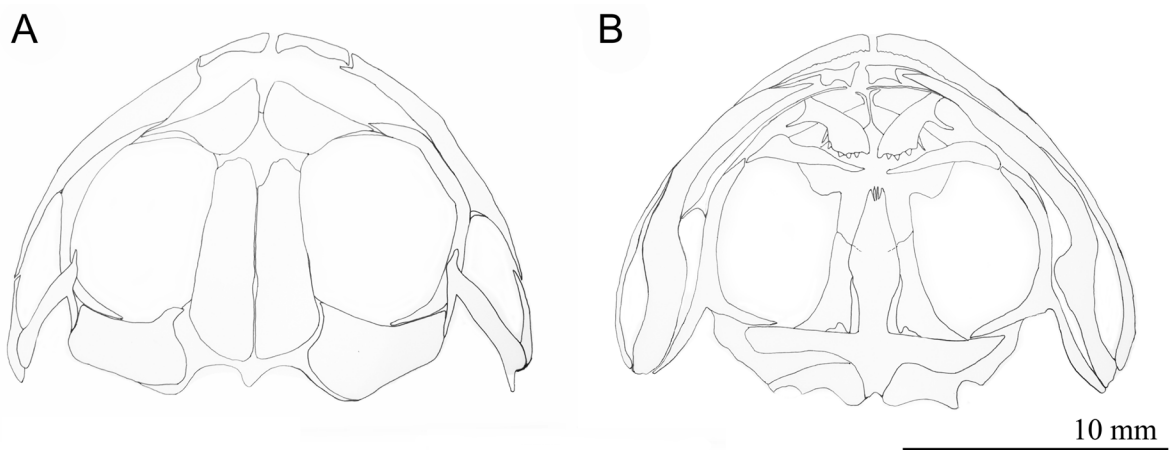

Fig. 6. *Odontophrynus toledoi* sp. nov. (ZUEC-AMP 23469), skull. **A**. Dorsal view. **B**. Ventral view.

Table 3. Measurements (in mm) and proportions of the holotype and five paratype males of *Odontophrynus toledoi* sp. nov. Values presented as mean ± sd, minimum–maximum values (range). See Material and methods for abbreviation definitions.

	Odontophrynus toledoi sp. nov.
MIL	47.16 ± 6.36 (35.81–52.91)
SKW	20.36 ± 1.8 (17.14–22.25)
SKL	14.71 ± 2.65 (9.57–17.02)
WFP	5.04 ± 0.59 (4.67–6.01)
LV2	2.39 ± 0.38 (1.87–2.8)
LSV	2.74 ± 0.69 (1.69–3.64)
SDW	8.87 ± 1.3 (7.79–10.9)
SKW/MIL	0.43 ± 0.03 (0.4–0.48)
SKL/MIL	0.31 ± 0.04 (0.27–0.38)
SKW/SKL	1.41 ± 0.19 (1.24–1.79)
LV2/MIL	0.05 ± 0.01 (0.04–0.06)
LSV/MIL	0.06 ± 0.01 (0.04–0.08)

Table 4. Advertisement call parameters of *Odontophrynus toledoi* sp. nov. including sampled populations from the type locality São Francisco Xavier (SFX), Parque Estadual de Campos do Jordão (PECJ) and Santo Antônio do Pinhal (SAP). The results are presented as mean ± sd, minimum–maximum values (range).

	All sites	SFX (n = 10) Type locality	PECJ (n = 3)	SAP (n = 2)
Minimum frequency (Hz)	490 ± 76	516 ± 89	466 ± 34	430 ± 21
	(395–690)	(395–689)	(410–533)	(400–480)
Maximum frequency (Hz)	1187 ± 97	1219 ± 105	1139 ± 44	1165 ± 109
	(1033–1399)	(1052–1399)	(1033–1209)	(1033–1300)
Dominant frequency (Hz)	876 ± 83	901 ± 74	815 ± 43	895 ± 117
	(775–1033)	(775–1033)	(775–861)	(775–1031)
Call duration (ms)	607 ± 118	573 ± 131	677 ± 28	583 ± 125
	(438–831)	(440–831)	(601–742)	(439–743)
Pulses per call	62 ± 7.3	63 ± 6	66 ± 2	56 ± 2
	(43–82)	(49–82)	(62–70)	(43–70)
Pulse duration (ms)	5 ± 1	4 ± 0.5	6 ± 1	5 ± 0.05
	(4–8)	(3–6)	(5–8)	(4–6)
Interval between pulses (ms)	3 ± 0.8	3 ± 0.05	4 ± 0.05	4 ± 0.05
	(2–5)	(2–5)	(3–5)	(4–5)
Pulse rates (pulses/s)	107 ± 13.5	118 ± 12	99 ± 4.8	97 ± 5.2
	(89–132)	(96–132)	(89–141)	(89.5–107)

transverse process of the presacral II directed anteriorly; transverse processes of presacral II–IV broader and longer than those of presacral V–VIII. Sacral diapophyses moderated dilated. Pectoral girdle arciferal. Clavicle arched directed forward. Ischia well developed. Pubis calcified. Phalangeal formula of hand: 3-3-4-4. Phalangeal formula of foot: 3-3-4-5-4. Pelvic girdle V-shaped.
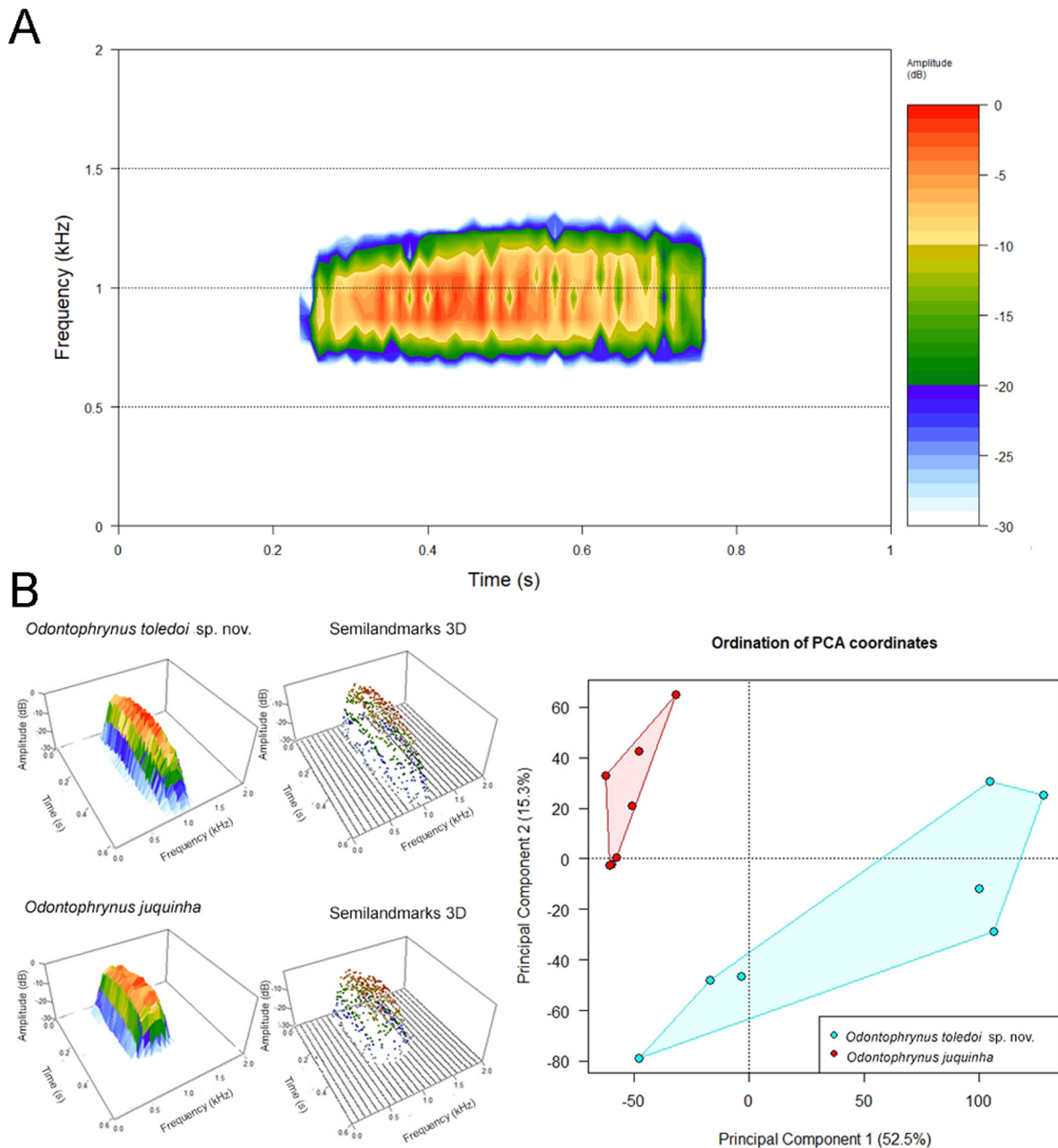

Fig. 7. A. Advertisement call of *Odontophrynus toledoi* sp. nov. **B**. Acoustic-space of *Odontophrynus toledoi* sp. nov. and *Odontophrynus juquinha* Rocha, Sena, Pezzuti, Leite, Svartman, Rosset, Baldo & Garcia, 2017, and the respective grid with the position of each semilandmark. The positions of the semilandmarks were obtained in the 3D spectrogram and summarized in a Principal Coordinate Analysis (PCA). With this, the ordering graphic recovered 73.8% of all the acoustic-space variance in the first two PCA axes, resulting in a non-overlapping of the acoustic-space of the two species.

Vocalization

The advertisement call of *Odontophrynus toledoi* sp. nov. (Fig. 7A) is characterized by a pulse group containing 43–82 pulses (average = 62 ± 7.3 pulses) occupying a frequency range between 395 and 1399 Hz and dominant frequency range 775 and 1033 (average = 876 ± 83 Hz). Call duration ranges from 438 to 831 ms (average = 607 ± 118 ms). Pulse duration ranges from 4 to 8 ms (average = 5 ± 1 ms) and interval between pulses is 3 ± 0.8 ms (2–5 ms). Pulse repetition rate ranges from 89 to 132 pulses per second (average = 107 ± 13.5 pulse/s) (Table 4). For complete comparisons between species see Table 5.

Karyotype

Odontophrynus toledoi sp. nov. is a tetraploid species, with 2n = 4X = 44, with all chromosomes biarmed (FN = 88). The karyotype is composed of five metacentric chromosome groups (1, 5–7, and 11) and six submetacentric chromosome groups (2–4 and 8–10; Fig. 8A). In cells in meiosis I, tetravalents were commonly seen, although in variable numbers (Fig. 8B). In Giemsa-stained metaphases, secondary constrictions were observed in the long arm of chromosomes 9, which corresponded to silver-stained NORs revealed by the Ag-NOR method. A notable variation was observed in NOR size in specimen ZUEC-AMP 24764. While three of its chromosomes 9 had large silver-stained NORs, which were easily seen as secondary constrictions in Giemsa-stained metaphases, one chromosome 9 had a small NOR (Fig. 8C), hardly seen in some metaphases. Such variation in NOR size justifies the differences observed in chromosome 9 length (Fig. 8A, C). Constitutive heterochromatin was detected in the centromeric region of all chromosomes (Fig. 8D).

Phylogenetic inferences and mitochondrial DNA divergences

Our gene tree for 16S mtDNA recovered the *Odontophrynus americanus* species group as monophyletic, with low support (0.77 posterior probability) and as a sister clade of the *O. occidentalis* and *O. cultripes* species group (*O. cultripes* and *O. carvalhoi*). Also, our gene tree recovered *Odontophrynus toledoi* sp. nov. as part of the *O. americanus* group (0.97 posterior probability). The clade of *O. americanus* group is composed by three small clades with the following relationship: *O. reigi* on the basis, as sister taxon of the remaining species, and (*O. cordobae* [*O. americanus* + *O. lavillai*]) as sister clade of (*O. toledoi* [*O. juquinha* + *O.* aff. *juquinha*]). The two delimitation analyses, bGMYC and BPP, were almost entirely congruent with each other, supporting the existence of nine and ten species, respectively, in the clade of the *Odontophrynus* spp. (Fig. 9), which mostly agrees with the current taxonomy of the group. Furthermore, the mitochondrial haplotype network shows that *O. toledoi* does not share haplotypes with other species of the *O. americanus* species group (Fig. 10).

Geographical distribution

The distribution of *Odontophrynus toledoi* sp. nov. comprises the southern portion of the Serra da Mantiqueira and adjacent areas that share species with the mountain range, such as Jundiaí and Atibaia in the state of São Paulo. The occurrence area covers two states in Brazil (São Paulo and Minas Gerais; Fig. 10). The type locality is São Francisco Xavier (SFX; district of the municipality of São José dos Campos, São Paulo) in the 'Rio Manso' area. The species can also be found in the Projeto Dacnis private reserve and in other flooded areas within the district. In the state of São Paulo, the municipalities of Campos do Jordão (Parque Estadual de Campos do Jordão (Horto Florestal), Santo Antônio do Pinhal (RPPN Fazenda Renópolis) São Bento do Sapucaí, Caçapava, Pindamonhangaba, Piquete and Queluz (Martins, I.A. pers. com.) are also in its range. In the state of Minas Gerais, the species can be found in the municipalities of Airuoca, Itamonte, Cristina (Mata da Prefeitura; Fazenda Pouso Frio), Maria da Fé (Fazenda Pomária), Poços de Caldas, Rio Preto, Inconfidentes and Marmelópolis.
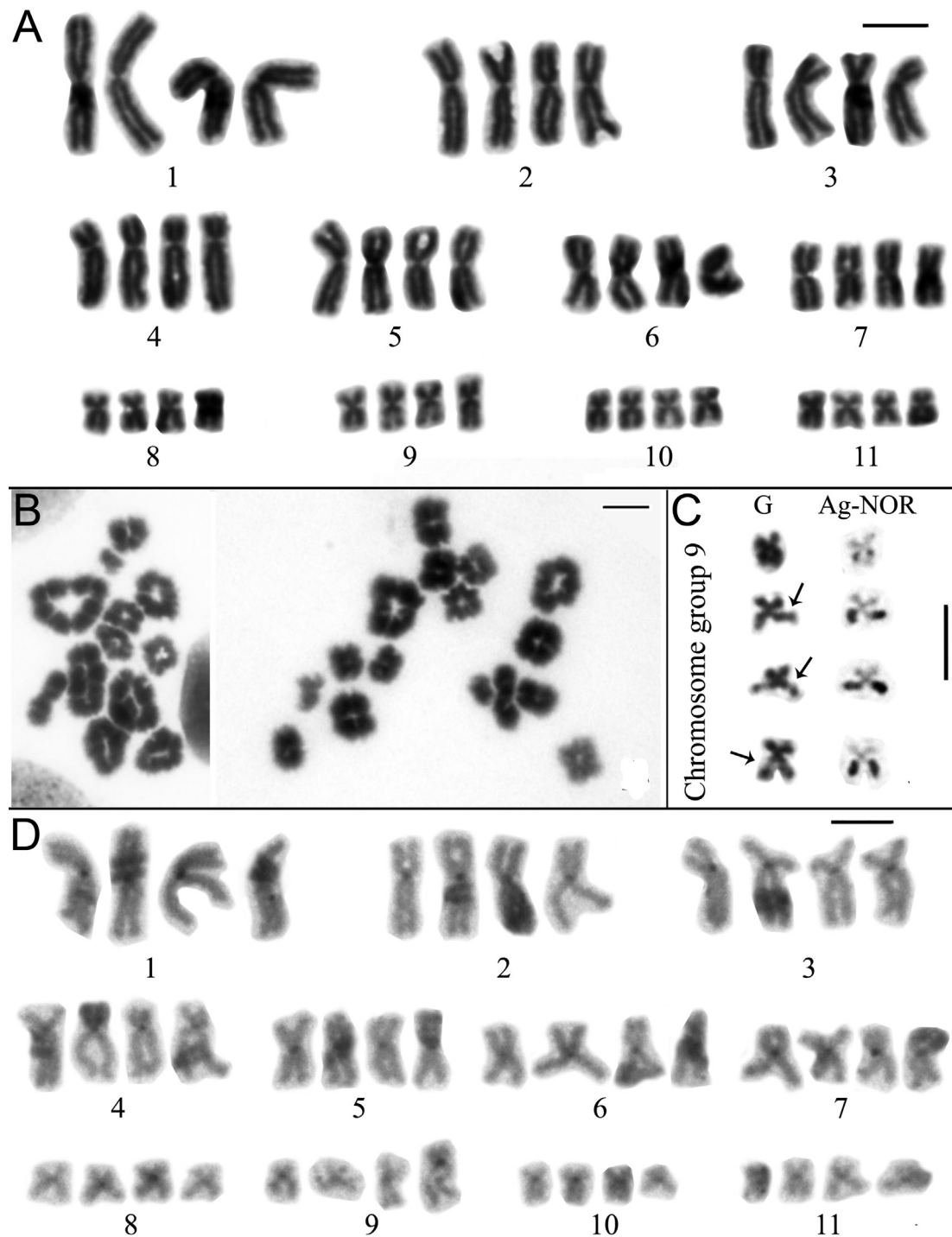
Fig. 8. Karyotype of *Odontophrynus toledoi* sp. nov. **A**. Giemsa-stained karyotype. Note the length variation among chromosomes 9 due to the NOR size variation (see text for details). **B**. Giemsa-stained chromosomes extracted from two distinct cells in meiosis I. The number of tetravalents differed between both cells. **C**. Chromosome group 9 from one metaphase of the specimen ZUEC-AMP 24764 sequentially subjected to Giemsa-staining (G) and the Ag-NOR method (Ag-NOR). Arrows indicate secondary constrictions. Note the NOR size variation among the homologues. **D**. C-banded karyotype. Scale bars = 10 µm.

Table 5. Advertisement calls of species from the *Odontophrynus americanus* group. Parameters presented as range.

Species	Call duration (ms)	Intercall interval (s)	Pulses/call	Pulse duration (ms)	Interval between pulses (ms)	Pulse rate (pulses/s)	Dominant frequency (Hz)	Reference
O. americanus	524–558	–	39–41	5.1–5.5	8–8.6	73–77	1025–1075	Martino & Sinsch 2002
O. cordobae	421–475	–	48–53	3.3–3.7	5.1–5.7	111–116	990–1040	Martino & Sinsch 2002
O. juquinha	322–610	–	32–62	5–8	3–6	90.5–106.7	840–1080	Rocha *et al.* 2017
O. lavillai	301.5–583	1.8–8.4	40–62	4.5–7	1.8–5	107.2–132.5	637.1–790.2	Rosset & Baldo 2014
O. maisuma	570–785	1.6–18.6	43–57	–	–	71.1–77.2	1124–1211	Borteiro *et al.* 2010
O. reigi	284.5–688.5	0.4–31.8	38–72	2.0–7.8	1.3–5.3	99.3–140.7	820–1121	Rosset *et al.* 2021
O. toledoi sp. nov.	438–831	–	43–82	4–8	2–5	89–132	775–1033	This work

Natural history

Odontophrynus toledoi sp. nov. is a terrestrial, nocturnal species commonly found in open and flooded areas. In the type locality (SFX), it was found mainly in valleys. In these locations, ephemeral wetlands receive more water from rivers and precipitation, especially during the rainy season (October–March). Although the frogs are predominantly nocturnal, they can also be heard during daylight on rainy days. They spend most of their time buried in aestivation and generally only come out after heavy rains. We also observed that females leave the aestivation period before males. Females emerge from holes approximately 7cm deep at the beginning of the rains, while males are only observed when there is a greater accumulation of precipitation.
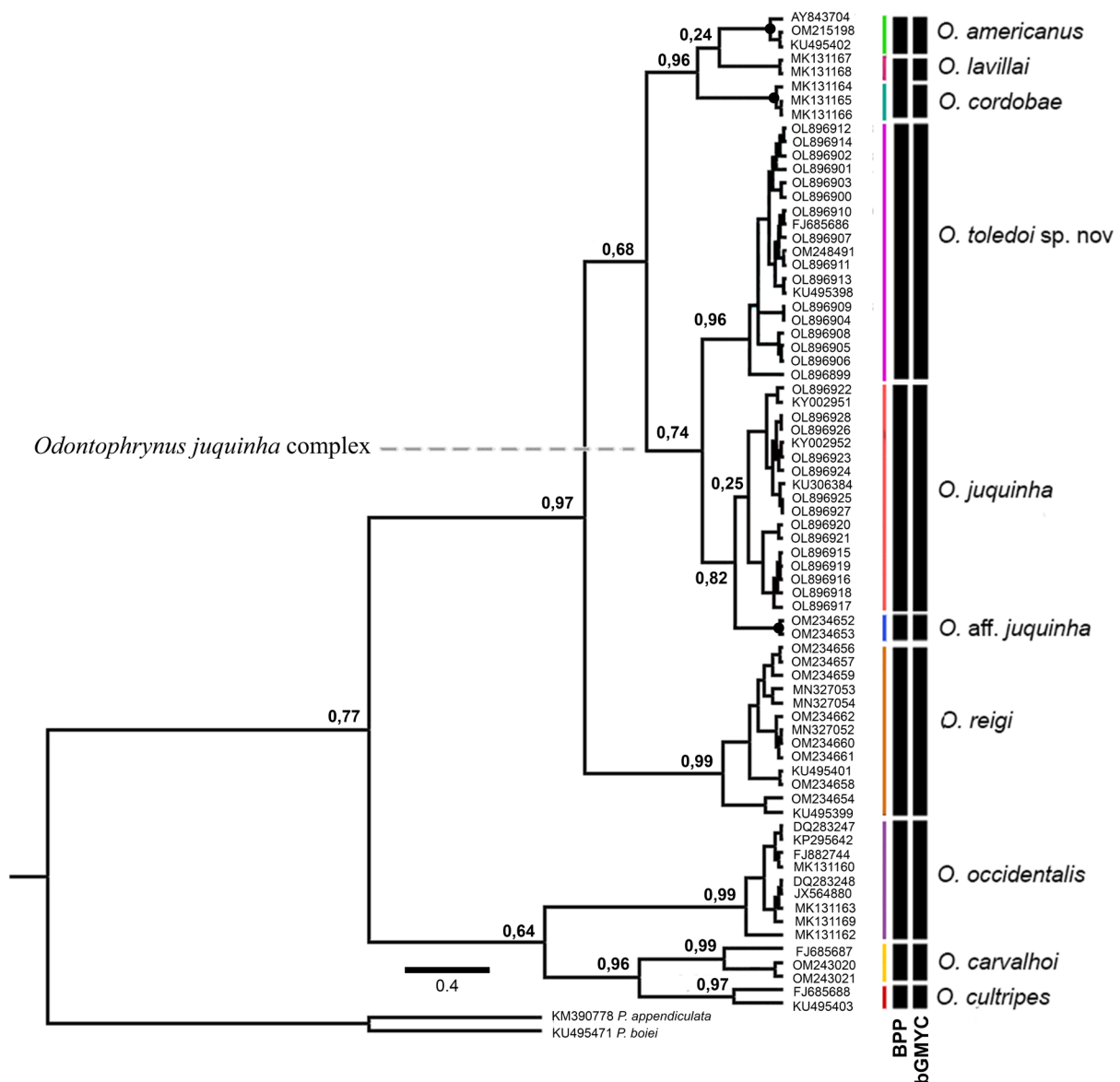

Fig. 9. Phylogenetic analysis of partial sequences of the 16S mtDNA gene of 10 species of the genus *Odontophrynus* Reinhardt & Lütken, 1862. Nodes are labeled with the Bayesian posterior probability. Scale bar (0.4) in million years. The black bars on the side represent the species delimitated by the bGMYC and BPP methods. The colored bars represents the haplotype groups shown and map in Fig. 10.
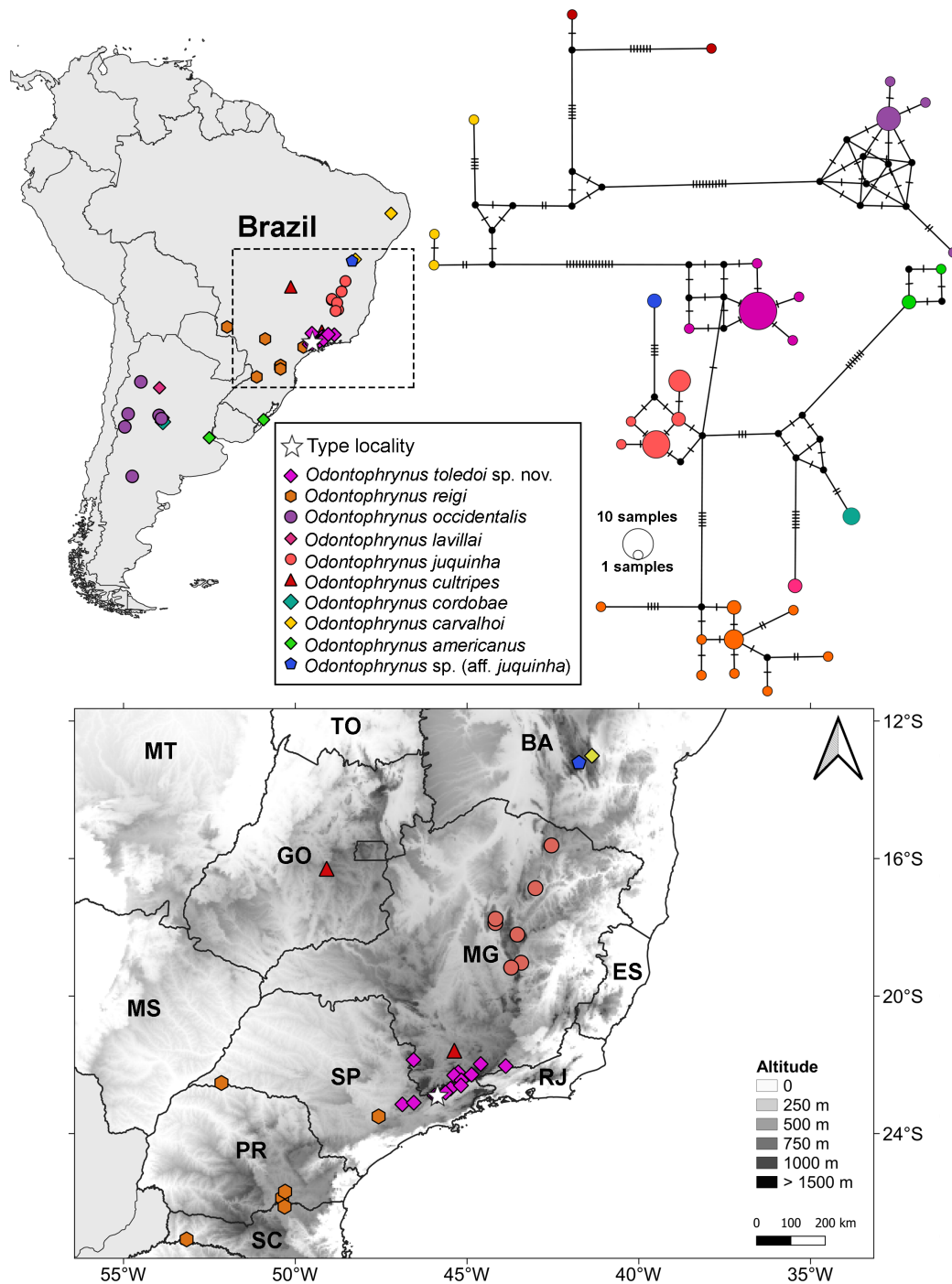
Fig. 10. Geographical distribution of ten species of *Odontophrynus* Reinhardt & Lütken, 1862 in South America and the respective haplotype network with the colors of each cluster also indicated on the map. Median-joining haplotype network of specimens from genus *Odontophrynus* based on partial sequences of the 16S mtDNA gene. Each haplotype is represented by a circle whose area is proportional to its frequency. Traits indicate additional mutational steps for branches with more than one mutation. Different colors indicate species-level units. The black dots are median vectors (hypothesized sequences). Highlighted, the altitude map shows the distribution of the genus in central, south, and southeast of Brazil. Abbreviations: BA = Bahia; ES = Espirito Santo; GO = Goiás; MS = Mato Grosso do Sul; MT = Mato Grosso; PR = Paraná; RJ = Rio de Janeiro; SC = Santa Catarina; SP = São Paulo; TO = Tocantins.

When noticing our presence, the species exhibited the defensive behaviors of burrowing (Fig. 11A–B), puffing up the body, stiff leg (Fig. 11C). Thanatosis occurred when they were handled. The species' coloration also provides camouflage in its environment (Fig. 11D). It is an explosive breeder and males cluster around temporary pools. Adult males can be seen calling with the body partially submerged in flooded areas, hidden in vegetation. The amplexus is axillary. Tadpoles are exotrophic, benthonic and inhabit mainly lentic environments, such as temporary ponds (ecomorphological guild II: A: 1; sensu Altig & McDiarmid 1999).

Comparison with other species

Odontophrynus toledoi sp. nov. is clearly distinguished from the species of the *O. cultripes* group (*O. cultripes*, *O. carvalhoi*, and *O. monachus*) and *O. occidentalis* by the absence of distinctly enlarged postorbital, temporal, and parotoid glandular warts (three or more pairs of enlarged rounded-oval postorbital, temporal, and parotoid glandular warts in *O. cultripes* and *O. occidentalis* species groups).

Odontophrynus toledoi sp. nov. is distinguished from *O. maisuma* by its smaller adult females SVL (37.9–43.6 mm in *O. maisuma*; Rosset 2008). From *O. americanus*, *O. cordobae* and *O. lavillai*, *O. toledoi* can be differentiated by the sloping snout in lateral view (truncate or obtuse in *O. americanus* [Martino & Sinsch 2002; present study] and truncate, poor sloping, in *O. lavillai* [Rosset *et al.* 2009]). *Odontophrynus toledoi* can be distinguished from *O. lavillai*, *O. maisuma* and *O. reigi* by the presence of fringes on fingers (absent in these species; Rosset 2008; Rosset *et al.* 2021), also from *O. maisuma* by the presence of fringes on toes (absent in this species; Rosset 2008). The new species can be distinguished from
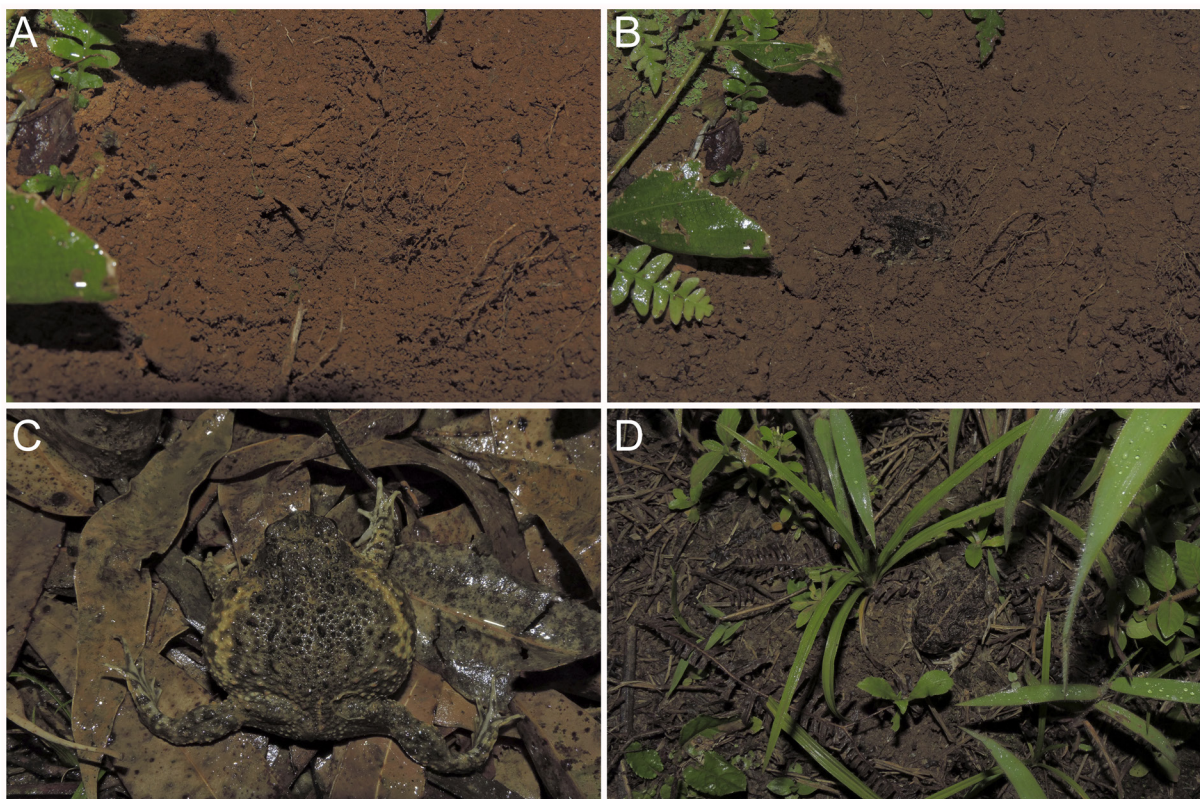

Fig. 11. *Odontophrynus toledoi* sp. nov. displaying defensive behaviors (**A–B**) of burrowing and (**C**) puffing up the body and stiff leg synergistically. **D**. The coloration of the species also provides crypsis by camouflage in the microhabitat where it lives.

O. cordobae, *O. juquinha*, *O. lavillai* and *O. maisuma* by having longitudinally oriented dorsal glandular ridges (scarce or absent in *O. cordobae*, *O. juquinha* and *O. lavillai*, and scarce or absent, except on postorbital and parotoid regions in *O. maisuma*), from *O. cordobae* by having the rostral glandular wart well developed (poorly developed or absent in *O. cordobae*), from *O. reigi* by the eye-nostril glandular wart poorly developed or absent (well developed in *O. reigi*). The skin texture of densely scattered big warts on dorsum can distinguish *O. toledoi* from *O. lavillai* (small warts scattered on dorsum; Cei 1980; Rosset 2008). The new species can be distinguished from *O. americanus*, *O. cordobae* and *O. maisuma* by the presence of few distinct postorbital and parotoid glands undifferentiated from other glands (glands form a longitudinal ridge in *O. maisuma*, rounded and curved postorbital and parotoid glands or ridges on *O. americanus* and *O. cordobae*; Savage & Cei 1965; Martino & Sinsch 2002; Rosset 2008). *Odontophrynus toledoi* also differs from the others by the temporal gland undistinguishable from other glands (distinctly rounded temporal gland in both *O. americanus* and *O. cordobae*, and absent in *O. maisuma*; Savage & Cei 1965; Martino & Sinsch 2002; Rosset 2008). The toe length can distinguish *O. toledoi* from *O. maisuma* (toe I does not reach the subarticular tubercle of the toe II in *O. toledoi*, and toe I reaches the subarticular tubercle of the toe II in *O. maisuma*; Rosset 2008).

In general, external morphology of tadpoles of *O. toledoi* sp. nov. are very similar to other members of the *O. americanus* group, *O. cultripes* group, and *O. occidentalis* group. However, in comparison with members of the *O. cultripes* group (*O. carvalhoi*, *O. monachus*, *O. cultripes*), tadpoles of *Odontophrynus toledoi* differ by their larger size, TL = 42.91–56.18 mm at stages 37–40, against *O. monachus* (TL = 36.9 mm at stage 36; Menegucci *et al.* 2016), *O. cultripes* (TL = 41 mm at stage 37; Savage & Cei 1965; Nascimento *et al.* 2013), with exception of *O. carvalhoi* (TL = 58.59 at stage 34; Caramaschi 1979; Santos *et al.* 2017). By lateral and ventral emarginations on the oral disc (lateral in *O. monachus* and *O. carvalhoi*; absent in *O. cultripes*). By 1–2 submarginal papillae on the posterior labium of each side of the oral disc (5–9 grouped laterally in both labia in *O. monachus*; 2–3 on upper labium and 3 on lower labium in *O. carvalhoi*). Furthermore, differentiated from *O. monachus* by tip of tail acute (rounded in *O. monachus*), ventral tube positioned slightly below ventral margin (at ventral margin in *O. monachus*), by body rounded in lateral view (globular in *O. monachus*). It can also be diagnosed from *O. carvalhoi* by having the spiracle's inner wall with small distal portion free (fused in *O. carvalhoi*), LTRF 2(2)/3(1) (varies among 2/3(1) and 2(2)/3(1) in *O. carvalhoi*), and elliptical body in dorsal view (ovoid in *O. carvalhoi*).

In comparison with tadpoles of the *O. americanus* group (*O. maisuma*, *O. juquinha*, *O. cordobae*, *O. americanus*, *O. lavillai*), tadpoles of *O. toledoi* sp. nov. can be distinguished by their smaller size at same or near stages, TL = 42.91–56.18 mm, stages 37–40, *O. maisuma* (TL = 47 mm at stages 33–36; Borteiro *et al.* 2010), *O. cordobae* (TL = 35.9–50.9 mm at stage 37; Grenat *et al.* 2009), *O. lavillai* (TL = 55.8 mm at stage 37; see Lavilla & Scrocchi 1991; Fabrezi & Vera 1997; Nascimento *et al.* 2013), except by being larger than *O. juquinha* (TL = 24.3–35.7 mm at stages 30–38; Rocha *et al.* 2017) and *O. americanus* (TL = 42 mm, stages 38–39; see Fernández & Fernández 1921; Fabrezi & Vera 1997; Nascimento *et al.* 2013). By body rounded in lateral view and elliptical in dorsal view (globular and ovoid in *O. maisuma*, *O. juquinha;* ovoid in dorsal view in *O. cordobae*; globular in dorsal view in *O. lavillai* and *O. americanus*). By by 1–2 submarginal papillae on the posterior labium (4–8 in both sides of oral disc in *O. juquinha*; 1–2 submarginal papillae lower/posterior lip in *O. cordobae*). By lateral and ventral emarginations on the oral disc (lateral in *O. juquinha*, *O. maisuma*, and lateral and subterminal in *O. cordobae*). By nostrils with small projection on marginal rim (absent in *O. maisuma*, *O. cordobae*). Moreover, differentiated from *O. juquinha* by vent tube with posterior portion free (entirely fused in *O. juquinha*). It can also be diagnosed from *O. maisuma* by having the spiracle's inner wall with small distal portion free (fused in *O. maisuma*), by having one-single row of papillae (varies from 1–2 rows on anterior/posterior labium in *O. maisuma*), and by tip of tail acute (rounded in *O. maisuma*).

Tadpoles of *O. toledoi* sp. nov. can be diagnosed from *O. occidentalis* (*O. occidentalis* group) by being smaller (*O. toledoi* TL = 42.91–56.18 mm, stages 37–40, *O. occidentalis* TL = 74 mm at stage 37; Savage & Cei 1965; Cei 1987), by one-single row of marginal papillae (two-rows along oral disc in *O. occidentalis* according to Nascimento *et al.* 2013). However, *O. barrioi* (González *et al.* 2014) synonym of the *O. occidentalis* (see Martino *et al.* 2019) have one-single row of marginal papillae. Furthermore, *O. toledoi* can be distinguished from species of the *O. occidentalis* group by its spiracle's inner wall with small distal portion free (inner wall absent in *O. occidentalis*/*O. barrioi*); and by its acute tip of tail (rounded in *O. barrioi* / acute in *O. occidentalis*; see Martino *et al.* 2019). These phenotypic variations may be due to plastic responses to environments and predators (Van Buskirk *et al.* 1997; Van Buskirk & McCollum 1999) as mentioned by Nascimento *et al.* (2013) and Martino *et al.* (2019). *Odontophrynus toledoi* can be distinguished from *O. maisuma* and *O. reigi* by: (1) phalangeal formula of hand and the foot (*O. toledoi* has one additional bone in each phalange, compared to other species); (2) skull with the termination of the cultriform process ending in four cusps (two cusps in both *O. maisuma* and *O. reigi*); (3) frontoparietal fontanelle not exposed (exposed in *O. maisuma*); (4) nasals and frontoratietal well separated (slightly separated in *O. reigi*).

The first two eigenvectors of the PCA describe 79.5 percent of the total variation present on tadpoles' morphological measures. PC1 show that tadpole of *O. toledoi* sp. nov. is not associated with any negative or positive axis, while in PC2 *O. toledoi* is associate to negative axis. However, PCA show non-overlapping between tadpoles of the genus *Odontophrynus* in comparison with tadpole of *O. toledoi* mainly when compared to *O. juquinha* (more close-related phylogenetically; Fig. 9). Also, shows that close-related species occupied distinct positions, and *O. maisuma* and *O. juquinha* are morphologically more distant from the *O. toledoi* (Fig. 12).

The advertisement call of *O. toledoi* sp. nov. distinguishes it from *O. americanus* by the lower interval between pulses (*O. toledoi* IBP = 2–5 ms; *O. americanus* 8–8.6 ms) and the higher number of pulses/call (*O. toledoi* P/C = 43–82; *O. americanus* 39–41). Moreover, *O. toledoi* differs from *O. cordobae* by the longer call duration (*O. toledoi* CD = 438–831 ms; *O. cordobae* 421–475 ms), by the higher number of pulses/call (*O. toledoi* P/C = 43–82; *O. cordobae* 48–53) and by its pulse duration (*O. toledoi* PD = 4–8 ms; *O. cordobae* 3.3–3.7 ms). *Odontophryns toledoi* – calls in the air temperature range of 18–20°C – is distinguished from *O. juquinha* and *O. lavillai* by the higher call duration (*O. toledoi* CD = 438–831 ms; *O. juquinha* 322–610 ms, air temperature 19.2°C; *O. lavillai* 301.5–583 ms, air temperature range 23–27°C). *Odontophryns toledoi* differs from *O. maisuma* by the lower dominant frequency (*O. toledoi* DF = 775–1033 Hz; *O. maisuma* 1124–1211 Hz). Furthermore, *O. toledoi* can be distinguished from *O. reigi* by the longer call duration (*O. toledoi* CD = 438– 831 ms; *O. reigi* 284.5–688.5 ms).

The first two eigenvectors of the PCA describe 73.8% of the total variation present on the acoustic traits of *Odontophrys toledoi* sp. nov. and *O. juquinha*, indicating a separate structuring in the advertisement call of the two species in the acoustic-space (Fig. 7B).

Lastly, the new species differs from *O. carvalhoi*, *O. cordobae*, *O. cultripes*, *O. juquinha*, *O. lavillai*, *O. maisuma*, *O. occidentalis*, and *O. reigi* by being tetraploid (all these species are diploid, with 2N = 22; Saez & Brum-Zorrilla 1966; Becak & Becak 1974; Salas & Martino 2007; Borteiro *et al.* 2010; Rocha *et al.* 2017; Rosset *et al.* 2021). Additionally, the new species differs from *O. cordobae*, *O. juquinha*, *O. maisuma* and *O. reigi* by having secondary constriction on the chromosomes of group 9, while in these species this is present at pair 4.

Discussion

We described a new species of *Odontophrynus* within the *O. americanus* group based on multiple lines of evidence, such as external morphology (adults and tadpole), osteology, molecular data,

karyotype, and acoustic attributes. On the basis of the 16S tree, this new species is sister to the clade (*O. juquinha* + *Odontophrynus* sp. [aff. *juquinha*]). The use of this gene in the present work suggests possible phylogenetic relationships and genetic distance that comprise a reliable line of evidence with the corroboration of other data for an integrative approach (see Padial *et al.* 2010). Morphology is maintained across the lineages, as in other species of the Odontophrynidae family, which can lead to subtle differences between closely related species (Rocha *et al.* 2017; Rosset *et al.* 2021; Santana *et al.* 2021). On the other hand, differences in karyotypes can result in reproductive isolation, being generally associated with distinctions in geographic distribution and acoustic parameters (Wasserman 1970; Stöck 1998; Martino & Sinsch 2002; Holloway *et al.* 2006; Rocha *et al.* 2017). In addition, we found that the clade species of *O. toledoi* sp. nov. occur in different biogeographic units. *Odontophrynus toledoi* is restricted to the Atlantic Forest of Serra da Mantiqueira, while *O. juquinha* is restricted to the Serra do Espinhaço savanna. Both mountain ranges are notable for their high number of endemic amphibian species (Cruz & Feio 2007; Silva *et al.* 2018). Another evidence is that, although the raw acoustic
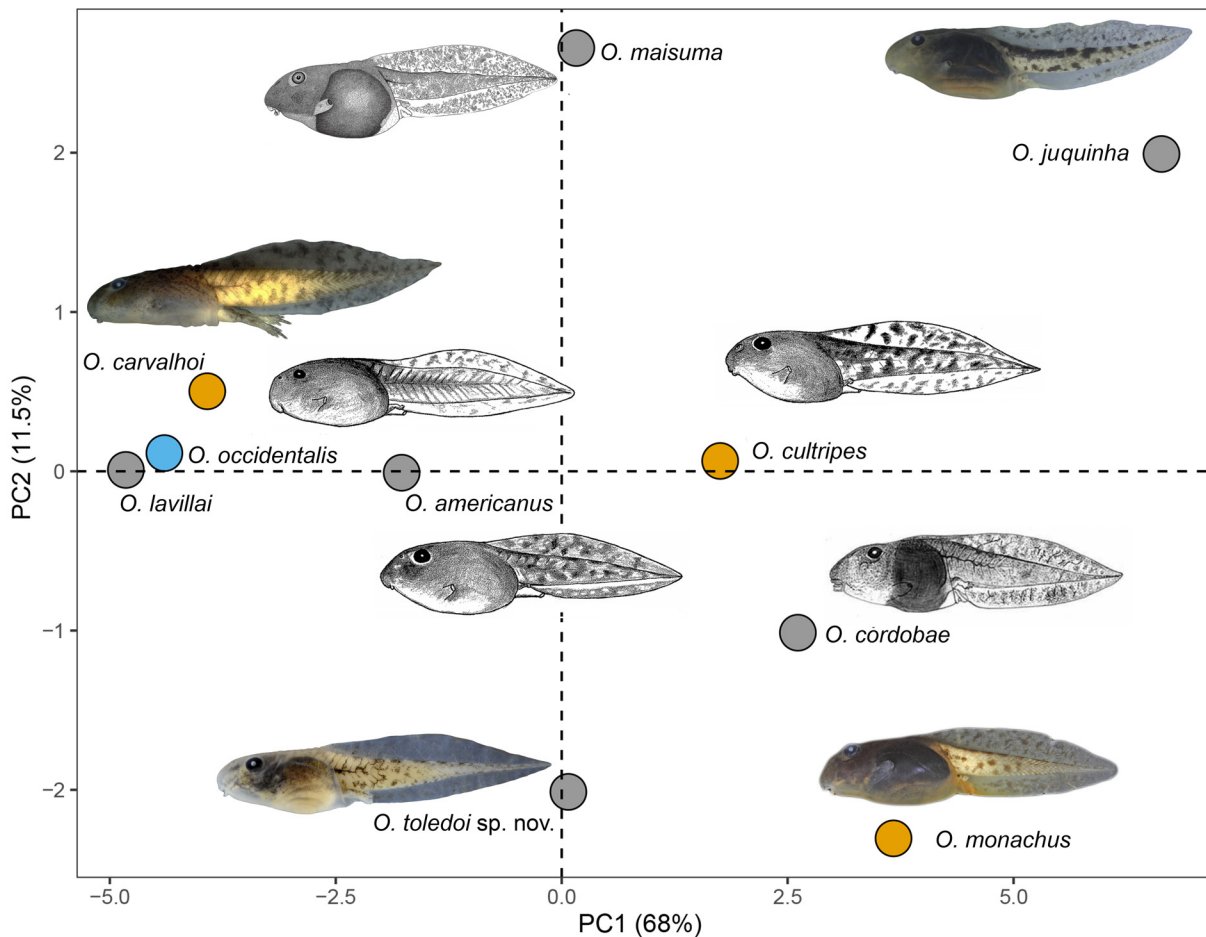

Fig. 12. Principal component analysis (PCA) of the linear measures showing distribution of the species in the reduced space composed by the first two principal components. Yellow circle = *O. cultripes* group, grey circle = *O. americanus* group, and blue circle = *O. occidentalis* group. Tadpole illustrations and pictures were obtained from the original species descriptions: *O. juquinha* image obtained from Rocha *et al.* 2017; *O. maisuma* image, from Borteiro *et al.* 2010; *O. monachus* image, from Menegucci *et al.* 2016; *O. carvalhoi* image, from Santos *et al.* 2017; *O. americanus*, *O. cultripes*, and *O. occidentalis*, from Savage & Cei 1965; and *O. cordobae* image, from Grenat *et al.* 2009). Linear measures used to perform PCA are in the Supp file 1: Table S2.

parameters of *Odontophrynus toledoi* and *O. juquinha* overlap at the limits of the ranges, we found a clear difference in the acoustic space structure. These reasons, taken together, reinforce the reproductive isolation between the two lineages and add another recognized species to a genus that is restricted to southeastern Brazil.

We also added the osteological description of another species of *Odontophrynus* to the body of knowledge about the genus. In the *O. americanus* species group, only *O. maisuma* and *O. reigi* have their osteological structures described, and now *O. toledoi* sp. nov. (Rosset 2008; Rosset *et al.* 2021). We couldn't compare *O. toledoi* with *O. juquinha* because no osteology analysis was made of the latter. However, we reinforce the need for osteological characters in taxonomic and systematic studies, since some osteological features can be extremely well preserved, particularly in the skull (Trueb 1977; Duellman & Trueb 1994). This is especially true in the genus *Odontophrynus*, which was first defined using skull osteological features alongside external morphology (Lynch 1971). The use of CT scans for osteological description provides the advantage of a non-invasive method, which can be applied in rare or even extinct species and also allows deeper reexamination of type specimens. However, this method is resolution-limited by the tomograph, which can determine the possibility of seeing or not small structures and forms, especially in the skull.

Two putative species within *Odontophrynus* had already been suggested by Martino *et al.* (2019): *O.* aff. *americanus* 2, which was described as *O. reigi* by Rosset *et al.* (2021), and *O.* aff. *americanus* 1, which we are describing now. Currently, the *Odontophrynus americanus* group comprises seven described species, five of which are diploid: *O. lavillai*, *O. cordobae*, *O. juquinha*, *O. maisuma*, and *O. reigi*; and two tetraploids: *O. toledoi* sp. nov. and *O. americanus*. The karyotype of *O. toledoi* was similar to that described by Beçak *et al.* (1966) for specimens from Campos do Jordão, São Paulo. Specimens from Campos do Jordão were also included in our molecular analyses and clustered together with topotypes *O. toledoi*, supporting the hypothesis that those sequences previously karyotyped by Beçak and collaborators belong to *O. toledoi*. The only difference between the karyotype we describe here and that described by Beçak *et al.* (1966) refers to the numbering of the smaller chromosomes. Probably, Beçak *et al.* (1966) disregarded the secondary constriction in the size analysis of the NOR-bearing chromosomes and considered that it was present in the short arm of chromosomes 11 (and not in the long arm of chromosomes 9, as we did). Although our cytogenetic study was based on males, Beçak and collaborators (1966) included males and females in their analyses, and heteromorphic sex chromosomes were not evidenced. Our study reinforces the importance of karyotypes for the diagnosis of species of *Odontophrynus*.

We found that *Odontophrynus toledoi* sp. nov., *O. juquinha* and *Odontophrynus* sp. (aff. *juquinha*) constitute a clade that is distributed along three different elevation areas in Brazil: Mantiqueira (*O. toledoi*) and Espinhaço (*O. juquinha*) ranges, and Chapada Diamantina (*Odontophrynus* sp. [aff. *juquinha*]). These three lineages corresponded to distinct haplogroups in the genetic analyses based on 16S rRNA partial gene and were recovered as independent evolutionary entities in the species delimitation tests. It is known that mountains constitute geographic barriers for several taxa, including frogs (Roberts *et al.* 2006; Vijayakumar *et al.* 2016). New studies should investigate how past climate may have influenced the speciation process of these three species. As they are associated with swampy areas and naturally exposed environments, they could be good models for understanding past connections of such different domains.

We observed that females leave the aestivation period before males. We suggest that this is likely due to greater investment in female reproduction, but this hypothesis still needs to be tested. Although the new species was found in at least 17 localities, wetlands are still constantly modified in the type locality by urbanization and water drainage for human use. These actions could be of conservation concern

for this species, since forested areas are more protected than naturally open environments. However, following the International Union for Conservation of Nature (IUCN) criteria, *O. toledoi* sp. nov. should be classified as Least Concern (LC) in spite of ongoing and potential habitat loss.

Acknowledgements

References

Altig R. & McDiarmid R.W. 1999. Body plan, development and morphology. *In*: McDiarmid R.W. & Altig R. (eds) *Tadpoles, the Biology of Anuran Larvae*: 24–51. University of Chicago Press, Chicago, IL.

Andrade F.S. de, Haga I.A., Ferreira J.S., Recco-Pimentel S.M., Toledo L.F. & Bruschi D.P. 2020. A new cryptic species of *Pithecopus* (Anura, Phyllomedusidae) in north-eastern brazil. *European Journal of Taxonomy* 723: 108–134. https://doi.org/10.5852/ejt.2020.723.1147

Araújo O.G.S., Toledo L.F., Garcia P.C.A. & Haddad C.F.B. 2009. Lista de anfíbios do estado de São Paulo. *Biota Neotropica* 9 (4): 197–209.

Becak M.L. & Becak W. 1974. Studies on polyploid amphibians: karyotype evolution and phylogeny of the genus *Odontophrynus*. *Journal of Herpetology* 8 (4): 337–341. https://doi.org/10.2307/1562903

Beçak M.L., Beçak W. & Rabello M.N. 1966. Cytological evidence of constant tetraploidy in the bisexual South American frog *Odontophrynus americanus*. *Chromosoma* 19 (2): 188–193. https://doi.org/10.1007/BF00293683

Blotto B.L., Pereyra M.O., Faivovich J., Dos Santos Dias P.H. & Grant T. 2017. Concentrated evolutionary novelties in the foot musculature of Odontophrynidae (Anura: Neobatrachia), with comments on adaptations for burrowing. *Zootaxa* 4258 (5): 425–442. https://doi.org/10.11646/zootaxa.4258.5.2

Borteiro C., Kolenc F., Pereyra M.O., Rosset S. & Baldo D. 2010. A diploid surrounded by polyploids: Tadpole description, natural history and cytogenetics of *Odontophrynus maisuma* Rosset from Uruguay (Anura: Cycloramphidae). *Zootaxa* 2611 (1): 1–15. https://doi.org/10.11646/zootaxa.2611.1.1

Bouckaert R.R. & Drummond A.J. 2017. bModelTest: Bayesian phylogenetic site model averaging and model comparison. *BMC Evolutionary Biology* 17 (1): 1–11. https://doi.org/10.1186/s12862-017-0890-6

Bouckaert R., Vaughan T.G., Barido-Sottani J., Duchêne S., Fourment M., Gavryushkina A., Heled J., Jones G., Kühnert D., De Maio N., Matschiner M., Mendes F.K., Müller N.F., Ogilvie H.A., Du Plessis L., Popinga A., Rambaut A., Rasmussen D., Siveroni I., Suchard M.A., Wu C.H., Xie D., Zhang C., Stadler T. & Drummond A.J. 2019. BEAST 2.5: an advanced software platform for Bayesian evolutionary analysis. *PLoS Computational Biology* 15 (4): e1006650. https://doi.org/10.1371/journal.pcbi.1006650

Caramaschi U. 1979. O girino de *Odontophrynus carvalhoi* Savage & Cei, 1965 (Amphibia, Anura, Ceratophrydidae). *Revista Brasileira de Biologia* 39 (1): 169–171.

Caramaschi U. & Napoli M.F. 2012. Taxonomic revision of the *Odontophrynus cultripes* species group, with description of a new related species (Anura, Cycloramphidae). *Zootaxa* 3155 (1): 1–20. https://doi.org/10.11646/zootaxa.3155.1.1

Cei J.M. 1980. *Amphibians of Argentina*. Vol. 2. Universitá degli studi di Firenze.

Cei J. 1985. Un nuevo y peculiar *Odontophrynus* de la sierra de Guasayán, Santiago del Estero, Argentina (Anura: Leptodactylidae). *Cuadernos de Herpetología* 1 (5): 1–13.

Cei J.M. 1987. Additional notes to Amphibians of Argentina: an update, 1980–1986. *Monitore Zoologico Italiano* 21 (3): 209–272.

Cianciarullo A.M., Bonini-Domingos C.R., Vizotto L.D., Kobashi L.S., Beçak M.L. & Beçak W. 2019. Whole-genome duplication and hemoglobin differentiation traits between allopatric populations of Brazilian *Odontophrynus americanus* species complex (Amphibia, Anura). *Genetics and Molecular Biology* 42 (2): 436–444. https://doi.org/10.1590/1678-4685-gmb-2017-0260

Colombo A.F. & Joly C.A. 2010. Brazilian Atlantic Forest lato sensu: The most ancient Brazilian forest, and a biodiversity hotspot, is highly threatened by climate change. *Brazilian Journal of Biology* 70 (3): 697–708. https://doi.org/10.1590/s1519-69842010000400002

Cruz C.A.G. & Feio R.N. 2007. Endemismos em anfíbios em áreas de altitude na Mata Atlântica no sudeste do Brasil. *In*: Nascimento L.B. & Oliveira M.E. (eds) *Herpetologia no Brasil II*: 117–126. Sociedade Brasileira de Herpetologia, Belo Horizonte, MG.

Drummond A.J. & Rambaut A. 2007. BEAST: Bayesian evolutionary analysis by sampling trees. *BMC Evolutionary Biology* 7 (1): 1–8. https://doi.org/10.1186/1471-2148-7-214

Drummond A.J., Suchard M.A., Xie D. & Rambaut A. 2012. Bayesian phylogenetics with BEAUti and the BEAST 1.7. *Molecular Biology and Evolution* 29 (8): 1969–1973. https://doi.org/10.1093/molbev/mss075

Duellman W. & Trueb L. 1994. *Biology of Amphibians*. The Johns Hopkins University Press, Baltimore, MD.

Duméril A.M.C. & Bibron G. 1841. *Erpétologie Genérale ou Histoire Naturelle Complète des Reptiles*. Vol. 8. Roret, Paris. https://doi.org/10.5962/bhl.title.45973

Edgar R.C. 2004. MUSCLE: Multiple sequence alignment with high accuracy and high throughput. *Nucleic Acids Research* 32 (5): 1792–1797. https://doi.org/10.1093/nar/gkh340

Fabrezi M. & Vera R. 1997. Caracterización morfológica de larvas de anuros del noroeste argentino. *Cuadernos de herpetología* 11 (1–2): 37–49.

Fernández K. & Fernández M. 1921. Sobre la biología y reproducción de algunos batracios argentinos. I. Cystignathidae. *Anales de la Sociedad Científica Argentina* 91: 97–140.

Frost D.R. 2021. Amphibian Species of the World: an Online Reference. Version 6.1. Available from https://amphibiansoftheworld.amnh.org/ [accessed 24 Oct. 2022].

Gatto K.P., Mattos J. V., Senger K.R. & Lourenço L.B. 2018. Sex chromosome differentiation in the frog genus *Pseudis* involves satellite DNA and chromosome rearrangements. *Frontiers in Genetics* 9 (301): 1–12. https://doi.org/10.3389/fgene.2018.00301

González E., Galvani G., Sanabria E., Barrasso D., Alcalde L. & Quiroga L. 2014. The tadpole of *Odontophrynus barrioi* Cei, Ruiz, and Beçak, 1982 (Anura: Odontophrynidae): a comparison with the other tadpoles of the genus. *Acta Herpetologica* 9 (1): 15–23. https://doi.org/10.13128/Acta_Herpetol-12931

Gosner K.L. 1960. A simplified table for staging anuran embryos and larvae with notes on identification. *Herpetologica* 16 (3): 183–190.

Grenat P.R., Zavala Gallo L.M., Salas N.E. & Martino A.L. 2009. The tadpole of *Odontophrynus cordobae* Martino & Sinsch, 2002 (Anura: Cycloramphidae) from central Argentina. *Zootaxa* 2151 (1): 66–68.

Grosjean S. 2005. The choice of external morphological characters and developmental stages for tadpole-based anuran taxonomy: a case study in *Rana* (*Sylvirana) nigrovittata* (Blyth, 1855) (Amphibia, Anura, Ranidae). *Contributions to Zoology* 74 (1–2): 61–76. https://doi.org/10.1163/18759866-0740102005

Guindon S., Dufayard J.F., Lefort V., Anisimova M., Hordijk W. & Gascuel O. 2010. New algorithms and methods to estimate maximum-likelihood phylogenies: Assessing the performance of PhyML 3.0. *Systematic Biology* 59 (3): 307–321. https://doi.org/10.1093/sysbio/syq010

Heyer W.R., Rand A.S., Cruz C.A.G. da, Peixoto O.L. & Nelson C. 1990. Frogs of Boracéia. *Arquivos de Zoologia* 31 (4): 231–410.

Hoang D.T., Vinh L.S., Flouri T., Stamatakis A., Von Haeseler A. & Minh B.Q. 2018. MPBoot: Fast phylogenetic maximum parsimony tree inference and bootstrap approximation. *BMC Evolutionary Biology* 18 (1): 1–11. https://doi.org/10.1186/s12862-018-1131-3

Hoffman E.A. & Blouin M.S. 2000. A review of colour and pattern polymorphisms in anurans. *Biological Journal of the Linnean Society* 70 (4): 633–665. https://doi.org/10.1006/bijl.1999.0421

Holloway A.K., Cannatella D.C., Gerhardt H.C. & Hillis D.M. 2006. Polyploids with different origins and ancestors form a single sexual polyploid species. *The American Naturalist* 167 (4): E88–E101. https://doi.org/10.1086/501079

Howell W.M. & Black D.A. 1980. Controlled silver-staining of nucleolus organizer regions with a protective colloidal developer: a 1-step method. *Experientia* 36: 1014–1016. https://doi.org/10.1007/BF01953855

Josse J. & Husson F. 2016. missMDA: a package for handling missing values in multivariate data analysis. *Journal of Statistical Software* 70 (1): 1–31. https://doi.org/10.18637/jss.v070.i01

Juncá F.A., Funch L. & Rocha W. 2005. *Biodiversidade e Conservação da Chapada Diamantina*. First Edition. Ministério do Meio Ambiente, Brasília.

Kalyaanamoorthy S., Minh B.Q., Wong T.K.F., Von Haeseler A. & Jermiin L.S. 2017. ModelFinder: fast model selection for accurate phylogenetic estimates. *Nature Methods* 14 (6): 587–589. https://doi.org/10.1038/nmeth.4285

King M. & Rofe R. 1976. Karyotypic variation in the Australian gekko *Phyllodactylus mamoratus* (Gray) (Gekkonidae: Reptilia). *Chromosoma* 54: 75–87.

King M. 1980. C-banding studies in Australian hylid frogs: secondary constriction structure and the concept of euchromatin transformation. *Chromosoma* 80: 191–207. https://doi.org/10.1007/BF00331835

Köhler J., Jansen M., Rodríguez A., Kok P.J.R., Toledo L.F., Emmrich M., Glaw F., Haddad C.F.B., Rödel M.O. & Vences M. 2017. The use of bioacoustics in anuran taxonomy: theory, terminology, methods and recommendations for best practice. *Zootaxa* 4251 (1): 1–124. https://doi.org/10.11646/zootaxa.4251.1.1

Lannoo M.J. 1987. Neuromast topography in tadpoles. *Journal of Morphology* 191: 247–263. https://doi.org/10.1002/jmor.1051910203

Lavilla E.O. & Scrocchi G.J. 1986. Morfometría larval de los géneros de Telmatobiinae (Anura: Leptodactylidae) decArgentina y Chile. *Physis* 44: 39–43.

Lavilla E. O. & Scrocchi G. J. 1991. Aportes a la herpetofauna del Chaco argentino: II- Nuevos datos sobre *Odontophrynus lavillai* Cei, 1985 (Anura: Leptodactylidae). *Acta Zoologica Lilloana* 40: 33–37.

Leigh J.W. & Bryant D. 2015. POPART: full-feature software for haplotype network construction. *Methods in Ecology and Evolution* 6 (9): 1110–1116. https://doi.org/10.1111/2041-210X.12410

Lynch J.D. 1971. *Evolutionary Relationships, Osteology, and Zoogeography of Leptodactyloid Frogs*. University of Kansas Publications, Museum of Natural History, Lawrence, Kansas. Available from https://www.biodiversitylibrary.org/page/3662221 [accessed 24 Oct. 2022].

Lyra M.L, Haddad C.F.B. & Azeredo-Espin A.M.L. 2017. Meeting the challenge of DNA barcoding Neotropical amphibians: polymerase chain reaction optimization and new COI primers. *Molecular Ecology Resources* 17 (5): 966–980. https://doi.org/10.1111/1755-0998.12648

MacLeod N., Krieger J. & Jones K.E. 2013. Geometric morphometric approaches to acoustic signal analysis in mammalian biology. *Hystrix* 24 (1): 110–125. https://doi.org/10.4404/hystrix-24.1-6299

Magalhães F. de M., Brandão R.A., Garda A.A. & Mângia S. 2020. Revisiting the generic position and acoustic diagnosis of *Odontophrynus salvatori* (Anura: Odontophrynidae). *Herpetological Journal* 30 (4): 189–196. https://doi.org/10.33256/hj30.4.189196

Martino A.L., Dehling J.M. & Sinsch U. 2019. Integrative taxonomic reassessment of *Odontophrynus* populations in Argentina and phylogenetic relationships within Odontophrynidae (Anura). *PeerJ* 7: e6480. https://doi.org/10.7717/peerj.6480

Martino A.L. & Sinsch U. 2002. Speciation by polyploidy in *Odontophrynus americanus*. *Journal of Zoology* 257 (1): 67–81. https://doi.org/10.1017/S0952836902000663

Martins I.A. & Jim J. 2003. Bioacoustic analysis of advertisement call in *Hyla nana* and *Hyla sanborni* (Anura, Hylidae) in Botucatu, São Paulo, Brazil. *Revista Brasileira de Biologia* 63 (3): 507–516. https://doi.org/10.1590/S1519-69842003000300017

Menegucci R.C., Santos M.T.T., Magalhães R.F. de, Machado I.F., Garcia P.C.A. & Pezzuti T.L. 2016. The tadpole of *Odontophrynus monachus* Caramaschi & Napoli, 2012 (Amphibia, Anura: Odontophrynidae). *Zootaxa* 4161 (4): 549–553. https://doi.org/10.11646/zootaxa.4161.4.5

Muscat E., Stuginski D., Nunes I., Martins I., Augusto-Alves G, Vittorazzi S.E., Toledo L.F. & Moroti M.T. 2020. Update on the geographic distribution of three poorly known frog species in the Mantiqueira mountain range. *Herpetology Notes* 13: 573–577.

Nascimento F.A.C., Mott T., Langone J.A., Davis C.A. & Sá R.O. 2013. The genus *Odontophrynus* (Anura: Odontophrynidae): a larval perspective. *Zootaxa* 3700 (1): 140–158. https://doi.org/10.11646/zootaxa.3700.L5

Nguyen L.T., Schmidt H.A., Von Haeseler A. & Minh B.Q. 2015. IQ-TREE: a fast and effective stochastic algorithm for estimating maximum-likelihood phylogenies. *Molecular Biology and Evolution* 32 (1): 268–274. https://doi.org/10.1093/molbev/msu300

Padial J.M., Miralles A., De la Riva I. & Vences M. 2010. The integrative future of taxonomy review. *Frontiers in Zoology* 7: 16. https://doi.org/10.1186/1742-9994-7-16

Peixoto M.A., Guedes T.B., Silva E.T. da, Feio R.N. & Romano P.S.R. 2020. Biogeographic tools help to assess the effectiveness of protected areas for the conservation of anurans in the Mantiqueira mountain range, Southeastern Brazil. *Journal for Nature Conservation* 54: 125799. https://doi.org/10.1016/j.jnc.2020.125799

Pinheiro P.D.P., Pezzuti T.L. & Garcia P.C.A. 2012. The tadpole and vocalizations of *Hypsiboas polytaenius* (Cope, 1870) (Anura, Hylidae, Hylinae). *South American Journal of Herpetology* 7 (2): 123–133. https://doi.org/10.2994/057.007.0202

Pons J., Barraclough T.G., Gomez-Zurita J., Cardoso A., Duran D.P., Hazell S., Kamoun S., Sumlin W.D. & Vogler A.P. 2006. Sequence-based species delimitation for the DNA taxonomy of undescribed insects. *Systematic Biology* 55 (4): 595–609. https://doi.org/10.1080/10635150600852011

Pyron A.R. & Wiens J.J. 2011. A large-scale phylogeny of Amphibia including over 2800 species, and a revised classification of extant frogs, salamanders, and caecilians. *Molecular Phylogenetics and Evolution* 61 (2): 543–583. https://doi.org/10.1016/j.ympev.2011.06.012

R Core Team 2022. R: A language and environment for statistical computing, ver. 4.1.3. R Foundation for Statistical Computing, Vienna, Austria. Available from https://www.R-project.org/ [accessed 24 Oct. 2022].

Rannala B. & Yang Z. 2003. Bayes estimation of species divergence times and ancestral population sizes using DNA sequences from multiple loci. *Genetics* 164 (4): 1645–1656. https://doi.org/10.1093/genetics/164.4.1645

Reid N.M. & Carstens B.C. 2012. Phylogenetic estimation error can decrease the accuracy of species delimitation: a Bayesian implementation of the general mixed Yule-coalescent model. *BMC Evolutionary Biology* 12: 196. https://doi.org/10.1186/1471-2148-12-196

Roberts J.L., Brown J.L., May R. von, Arizabal W., Schulte R. & Summers K. 2006. Genetic divergence and speciation in lowland and montane peruvian poison frogs. *Molecular Phylogenetics and Evolution* 41 (1): 149–164. https://doi.org/10.1016/j.ympev.2006.05.005

Rocha P.C. & Romano P.S.R. 2021. The shape of sound: a new R package that crosses the bridge between bioacoustics and geometric morphometrics. *Methods in Ecology and Evolution* 12 (6): 1115–1121. https://doi.org/10.1111/2041-210X.13580

Rocha P.C., De Sena L.M.F., Pezzuti T.L., Leite F.S.F., Svartman M., Rosset S.D., Baldo D. & Garcia P.C. de A. 2017. A new diploid species belonging to the *Odontophrynus americanus* species group (Anura: Odontophrynidae) from the espinhaço range, Brazil. *Zootaxa* 4329 (4): 327–350. https://doi.org/10.11646/zootaxa.4329.4.2

Rohlf F.J. 2015. The tps series of software. *Hystrix* 26 (1): 1–4. https://doi.org/10.4404/hystrix-26.1-11264

Rohlf F.J. 2017. *tpsDig2, Digitize Landmarks and Outlines. Version 2.31.* Department of Ecology and Evolution, State University of New York at Stony Brook.

Rossa-Feres D.D.C., Sawaya R.J., Brasileiro C.A., Schiesari L., Nazareth J., Gallardo R.A., Aires B., Vista B., Claro R. & Artes E. De 2010. Anfíbios do Estado de São Paulo, Brasil: conhecimento atual e perspectivas. *Biota Neotropica* 11: 47–66.

Rosset S.D. 2008. New species of *Odontophrynus* Reinhardt and Lütken 1862 (Anura: Neobatrachia) from Brazil and Uruguay. *Journal of Herpetology* 42 (1): 134–144. https://doi.org/10.1670/07-088R1.1

Rosset S.D. & Baldo J.D. 2014. The advertisement call and geographic distribution of *Odontophrynus lavillai* Cei, 1985 (Anura: Odontophrynidae). *Zootaxa* 3784 (1): 79–83. https://doi.org/10.11646/zootaxa.3784.1.5

Rosset S.D., Baldo D., Lanzone C. & Basso N.G. 2006. Review of the geographic distribution of diploid and tetraploid populations of the *Odontophrynus americanus* species complex (Anura: Leptodactylidae). *Journal of Herpetology* 40 (4): 465–477. https://doi.org/dqq23p

Rosset S.D., Baldo D. & Haddad C.F.B. 2009. Amphibia, Anura, Cycloramphidae, *Odontophrynus lavillai*: first record for Brazil and geographic distribution map. *Check List* 5 (1): 32–34. https://doi.org/10.15560/5.1.32

Rosset S.D., Fadel R.M., da Silva Guimarães C., Carvalho P.S., Ceron K., Pedrozo M., Serejo R., dos Santos Souza V., Baldo D. & Mângia S. 2021. A new burrowing frog of the *Odontophrynus americanus* species group (Anura, Odontophrynidae) from subtropical regions of Argentina, Brazil, and Paraguay. *Ichthyology and Herpetology* 109 (1): 228–244. https://doi.org/10.1643/h2020056

Saez F.A. & Brum Zorrilla N. 1966. Karyotype variation in some species of the genus *Odontophrynus* (Amphibia-Anura). *Caryologia* 19 (1): 55–63. https://doi.org/10.1080/00087114.1966.10796204

Salas N. & Martino A. 2007. Karyotype of *Odontophrynus cordobae* Martino & Sinsch , 2002 (Anura, Leptodactylidae). *Journal of Basic and Applied Genetics* 18 (1): 1–5.

Santana D.J., da Silva L.A., Sant'Anna A.C., Shepard D.B. & Mângia S. 2021. A new species of *Proceratophrys* Miranda- Ribeiro, 1920 (Anura, Odontophrynidae) from Southern Amazonia, Brazil. *PeerJ* 9: e12012. https://doi.org/10.7717/peerj.12012

Santos D.L., Andrade S.P., Rocha C.F., Maciel N.M., Caramaschi U. & Vaz-Silva W. 2017. Redescription of the tadpole of *Odontophrynus carvalhoi* Savage and Cei, 1965 (Anura, Odontophrynidae) with comments on the geographical distribution of the species. *Zootaxa* 4323 (3): 419–422. https://doi.org/10.11646/zootaxa.4323.3.7

Savage J.M. & Cei J.M.A.M. 1965. A review of the leptodactylid frog genus, *Odontophrynus*. *Herpetologica* 21 (3): 178–195.

Savage J.M. & Heyer W.R. 1997. Digital webbing formulae for Anurans: a refinement. *Herpetological Review* 28 (3): 131.

Schmid M., Olert J. & Klett C. 1979. Chromosome banding in amphibia - III. Sex chromosomes in Triturus. *Chromosoma* 71 (1): 29–55. https://doi.org/10.1007/BF00426365

Silva E.T. da, Peixoto M.A.A., Leite F.S.F., Feio R.N. & Garcia P.C.A. 2018. Anuran distribution in a highly diverse region of the Atlantic Forest: the Mantiqueira Mountain Range in Southeastern Brazil. *Herpetologica* 74 (4): 294–305. https://doi.org/10.1655/0018-0831.294

Stöck M. 1998. Mating call differences between diploid and tetraploid green toads (*Bufo viridis* complex) in Middle Asia. *Amphibia Reptilia* 19 (1): 29–42. https://doi.org/10.1163/156853898X00313

Talavera G. & Castresana J. 2007. Improvement of phylogenies after removing divergent and ambiguously aligned blocks from protein sequence alignments. *Systematic Biology* 56 (4): 564–577. https://doi.org/10.1080/10635150701472164

Trueb L. 1977. Osteology and anuran systematics: intrapopulational variation in *Hyla lanciformis*. *Systematic Biology* 26 (2): 165–184. https://doi.org/10.1093/sysbio/26.2.165

Van Buskirk J. & McCollum S. A. 1999. Plasticity and selection explain variation in tadpole phenotype between ponds with different predator composition. *Oikos* 85: 31–39. https://doi.org/10.2307/3546789

Van Buskirk J., McCollum S.A. & Werner E.E. 1997. Natural selection for environmentally induced phenotypes in tadpoles. *Evolution* 51 (6): 1983–1992. https://doi.org/10.1111/j.1558-5646.1997.tb05119.x

Vijayakumar S.P., Menezes R.C., Jayarajan A. & Shanker K. 2016. Glaciations, gradients, and geography: Multiple drivers of diversification of bush frogs in the western ghats escarpment. *Proceedings of the Royal Society B: Biological Sciences* 283 (1836): 28320161011. https://doi.org/10.1098/rspb.2016.1011

Wasserman A.O. 1970. Polyploidy in the common tree toad *Hyla versicolor* Le Conte. *Science* 167: 385–386. https://doi.org/10.1126/science.167.3917.385

Watters J.L., Cummings S.T., Flanagan R.L. & Siler C.D. 2016. Review of morphometric measurements used in anuran species descriptions and recommendations for a standardized approach. *Zootaxa* 4072 (4): 477–495. https://doi.org/10.11646/zootaxa.4072.4.6

Supplementary file

Supp. file 1. Additional information. https://doi.org/10.5852/ejt.2022.847.1991.8119

Specimens examined.

Table S1. DNA samples of *Odontophrynus* Reinhardt & Lütken, 1862 used in this study.

Table S2. Comparative table of the morphological measures (in millimeters) present in the descriptions of tadpoles of the genus *Odontophrynus* Reinhardt & Lütken, 1862. Characters followed by an asterisk (*) were inferred from the pictures and illustrations (using TPSDig2), but not mentioned in the text by the authors. Cells marked with NA represent measures not available. All measures presented are the mean of each species mentioned in the text by the authors, except measures inferred from the pictures.